Quaternary Science Reviews 99 (2014) 97–111

Contents lists available at ScienceDirect

Quaternary Science Reviews

journal homepage: www.elsevier.com/locate/quascirev

Peak Last Glacial weathering intensity on the North American continent recorded by the authigenic Hf isotope composition of North Atlantic deep-sea sediments

Marcus Gutjahr [a, b, *], Martin Frank [b], Jörg Lippold [c, e], Alex N. Halliday [d]

[a] Institute for Isotope Geochemistry and Mineral Resources, Department of Earth Sciences, ETH Zürich, 8092 Zürich, Switzerland
[b] GEOMAR Helmholtz Centre for Ocean Research Kiel, Wischhofstrasse 1-3, 24148 Kiel, Germany
[c] Institute of Environmental Physics, University of Heidelberg, Heidelberg, Germany
[d] Department of Earth Sciences, University of Oxford, Parks Road, OX1 3PR Oxford, UK
[e] Oeschger Centre for Climate Change Research, Institute of Geological Sciences, University of Bern, Switzerland

ARTICLE INFO

Article history:
Received 29 January 2014
Received in revised form
30 April 2014
Accepted 16 June 2014
Available online

Keywords:
Authigenic hafnium
Fe–Mn oxyhydroxide
Laurentide Ice Sheet
Incongruent weathering
Zircon effect
Lu-rich accessory minerals
Feldspar weathering
Deglaciation
LGM

ABSTRACT

We have retrieved radiogenic hafnium (Hf) isotope compositions (ε_{Hf}) from authigenic Fe–Mn oxyhydroxides of deep northwest Atlantic sediments deposited over the past 26 ka to investigate the oceanic evidence of changes in dissolved weathering inputs from NE America during the last deglaciation. The extraction of seawater-derived Hf isotopic compositions from Fe–Mn oxyhydroxides is not a standard procedure. Comparisons between the Al/Hf ratios and Hf isotopic compositions of the chemically extracted authigenic phase on the one hand, and those of the corresponding detrital fractions on the other, provide evidence that the composition of past seawater has been reliably obtained for most sampled depths with our leaching procedures. This is endorsed most strongly by data for a sediment core from 4250 m water depth at the deeper Blake Ridge, for which consistent replicates were produced throughout. The Hf isotopic composition of the most recent sample in this core also closely matches that of nearby present day central North Atlantic seawater. Comparison with previously published seawater Nd and Pb isotope compositions obtained on the same cores shows that both Hf and Pb were released incongruently during incipient chemical weathering, but responded differently to the deglacial retreat of the Laurentide Ice Sheet. Hafnium was released more congruently during peak glacial conditions of the Last Glacial Maximum (LGM) and changed to typical incongruent interglacial ε_{Hf} signatures either during or shortly after the LGM. This indicates that some zircon-derived Hf was released to seawater during the LGM. Conversely, there is no clear evidence for an increase in the influence of weathering of Lu-rich mineral phases during deglaciation, possibly since relatively unradiogenic Hf contributions from feldspar weathering were superimposed. While the authigenic Pb isotope signal in the same marine sediment samples traced peak chemical weathering rates on continental North America during the transition to the Holocene a similar incongruent excursion is notably absent in the Hf isotope record. The early change towards more radiogenic ε_{Hf} in relation to the LGM may provide direct evidence for the transition from a cold-based to a warm-based Laurentide Ice Sheet on the Atlantic sector of North America.

1. Introduction

During the glacial cycles of the past 2.7 Ma, northern North America has recurrently been overlain by substantial continental ice in the form of the Laurentide Ice Sheet (LIS) (Dyke and Prest, 1987; Clark and Pollard, 1998; Lisiecki and Raymo, 2007). The LIS alone stored as much as 56–76 m of sea level equivalent during the LGM (Paterson, 1972; Peltier, 1994; Carlson and Clark, 2012). Despite its importance for northern hemisphere Pleistocene climate the areal extent and volume of the LIS during non-peak glacial conditions is not well understood. Furthermore, its growth and retreat should have generated variable runoff fluxes into the adjacent ocean basins, but these too are not well constrained. This lack of knowledge regarding intermediate-sized ice sheet evolution is largely due to loss of geomorphological and geochemical

* Corresponding author. GEOMAR Helmholtz Centre for Ocean Research Kiel, Wischhofstrasse 1-3, 24148 Kiel, Germany. Tel.: +49 431 600 2232; fax: +49 431 600 2928.
E-mail address: mgutjahr@geomar.de (M. Gutjahr).

http://dx.doi.org/10.1016/j.quascirev.2014.06.022
0277-3791/

evidence of these intermediate climate- and ice sheet states on land. As a result, the evolution of North American physicochemical weathering conditions and chemical runoff fluxes are not very well known for most of the recent Pleistocene geological history, although it is evident from the marine isotopic budgets of elements such as Sr that chemical weathering fluxes varied significantly on glacial–interglacial timescales (Vance et al., 2009).

In contrast to incomplete continental Pleistocene sedimentary sequences of continental North America, marine sediments in the northwest Atlantic adjacent to the LIS should have recorded an undisturbed and continuous geochemical LIS runoff history. Trace metals transferred in solution to the marine realm are scavenged from seawater and incorporated into authigenic phases (Bruland and Lohan, 2003). The isotopic compositions of some of these elements provide clues as to the conditions under which weathering and erosion took place. For example, the release of Pb during incipient chemical weathering of freshly eroded rocks is highly incongruent, meaning that its isotopic composition reflects that of more soluble minerals and of more loosely bound radiogenic Pb as a consequence of α-recoil processes rather than that of the bulk rocks. This is particularly true in recently deglaciated areas (Erel et al., 1994; Harlavan et al., 1998). The incongruent release is manifested in more radiogenic Pb isotopic compositions of the early Holocene North American runoff compared with corresponding bulk crustal Pb of the source rocks (e.g., Gutjahr et al., 2009; Crocket et al., 2013). The resultant seawater Pb isotope records archived in authigenic Fe–Mn oxyhydroxides of marine sediments of the last glacial–interglacial transition provided records of spatially and temporally resolved variations in runoff fluxes to the northwest Atlantic (Gutjahr et al., 2009; Kurzweil et al., 2010) and the Labrador Sea (Crocket et al., 2012). The pronounced radiogenic Pb isotope excursions facilitated the determination of early Holocene peak chemical weathering rates in the interior of northeast America and provided new constraints on the opening of the major eastern runoff route to the North Atlantic via the St. Lawrence seaway during the Younger Dryas (Kurzweil et al., 2010).

Hafnium is another radiogenic trace metal isotope system that is released incongruently during chemical weathering (Patchett et al., 1984; Piotrowski et al., 2000; van de Flierdt et al., 2002). Lutetium-176 decays to ^{176}Hf with a half life of 37.2 Ga (Scherer et al., 2001). Lutetium is a rare earth element (REE) whereas Hf is a high field strength element (HFSE) resulting in significantly different chemical affinities and partition coefficients into major and trace mineral phases during formation of continental crust. Just as radiogenic Pb isotopes trace preferential weathering of uranium- and/or thorium-rich mineral phases in recently deglaciated continental areas, Hf isotopes trace preferential weathering of Lu-rich and/or Lu-poor mineral phases (Bayon et al., 2006, 2012). The radiogenic Hf isotope ratio ($^{176}Hf/^{177}Hf$) is usually reported in the ε_{Hf} notation as deviation from the chondritic uniform reservoir (CHUR):

$$\varepsilon_{Hf} = \left[\frac{\left[{}^{176}Hf/{}^{177}Hf_{sample}\right]}{\left[{}^{176}Hf/{}^{177}Hf_{CHUR}\right]} - 1\right] \times 10^4$$

with $^{176}Hf/^{177}Hf_{CHUR} = 0.282772$ (Blichert-Toft and Albarède, 1997). Similarly, Nd isotopes are expressed as ε_{Nd} values relative to $^{143}Nd/^{144}Nd_{CHUR} = 0.512638$ (Jacobsen and Wasserburg, 1980).

Hafnium is highly depleted in open ocean seawater, reaching concentrations as low as 0.04 pmol/kg in surface waters of the Southern Ocean (Rickli et al., 2010; Stichel et al., 2012b). In contrast, surface water concentrations of up to 4.2 pmol/kg have been found in low salinity waters in the Arctic Ocean originating from riverine inputs (Zimmermann et al., 2009a). The majority of published open seawater Hf concentrations are below 1.5 pmol/kg (e.g., Godfrey et al., 2009; Rickli et al., 2009; Zimmermann et al., 2009b; Stichel et al., 2012a). Efficient removal of Hf in estuaries contributes to the low concentrations in seawater (Godfrey et al., 2008). Several publications discussing the Hf speciation and behaviour in seawater proposed a residence time for Hf longer than that of Nd (White et al., 1986; Godfrey et al., 1997, 2008). In contrast, despite the relative Hf isotopic similarity in the various ocean basins, recent water column work suggests a short residence time of Hf in seawater based largely on the chemical behaviour and scavenging intensity, as well as the lack of enrichment in dissolved deep water Hf concentrations along the flow paths of deep water masses in the Atlantic (Rickli et al., 2009; Rickli et al., 2010, 2014; Chen et al., 2013a). The latter view implies that the deep marine ε_{Hf} signature is mainly controlled by proximal (intra-basin) weathering contributions largely independent of the origin of prevailing deep water masses.

Since a large proportion of continental Hf is stored in the mineral zircon, which is hardly accessible during non-glacial chemical weathering (cf. Rickli et al., 2013), the corresponding continental runoff signal is offset to more radiogenic ε_{Hf} signatures than the bulk crustal Hf isotope signal. Albarède et al. (1998) coined the term *seawater array* for this systematic offset towards more radiogenic ε_{Hf} for a given ε_{Nd} in seawater-derived hydrogenetic ferromanganese deposits than in bulk terrestrial rocks. The seawater array was confirmed in subsequent studies using hydrogenetic Fe–Mn crusts (e.g. Piotrowski et al., 2000; David et al., 2001) and direct seawater measurements (e.g., Godfrey et al., 2009; Rickli et al., 2009; Zimmermann et al., 2009b; Stichel et al., 2012a). More recently, chemical weathering of either lutetium-rich mineral phases or rather unradiogenic feldspars were proposed to contribute significantly to the observed shift (Bayon et al., 2006, 2012; Chen et al., 2011). Some authors also argued that the offset towards more radiogenic ε_{Hf} of seawater or at least some level of decoupling between hydrogenetic ε_{Hf} and ε_{Nd} (van de Flierdt et al., 2004) is controlled by significant contributions of hydrothermal Hf characterised by highly radiogenic mantle-like isotope signatures (White et al., 1986; Bau and Koschinsky, 2006). While hydrothermal inputs may indeed contribute to the Hf budget of seawater, a strong continental source is clearly required in order to explain the Hf isotopic differences between the ocean basins (van de Flierdt et al., 2007; Chen et al., 2013b). Therefore, seawater-derived ε_{Hf} in northwest Atlantic sediments is expected to reflect changes glacial weathering conditions in North America given the Hf residence time well below the average ocean mixing time (cf. Piotrowski et al., 2000; van de Flierdt et al., 2002).

This study investigates the Hf isotope evolution of northwest Atlantic deep water during the last glacial–interglacial transition. Seawater-derived colloidal or truly dissolved Hf is incorporated into the authigenic Fe–Mn oxyhydroxide phase of marine pelagic sediments (Chen et al., 2012). Since Hf is depleted both in seawater and in marine authigenic Fe–Mn oxyhydroxides, the extraction of a pure seawater-derived Hf phase from sediments is less straightforward than for example for Nd, Pb, or Th (Bayon et al., 2002; Gutjahr et al., 2007; Robinson et al., 2008; Basak et al., 2011). Our findings demonstrate both the potential but also the limitations associated with the extraction of a seawater Hf isotope signature from marine drift sediments. Following a critical assessment of the chemical and isotopic composition of the chemically extracted authigenic fraction of Hf, the isotopic records are compared with previously published authigenic Pb and Nd isotope records from the same sediment cores (Gutjahr et al., 2008, 2009). In combination with these other records, it is possible to constrain whether variations in deep water ε_{Hf} have been controlled by chemical weathering trends alone, by changes in provenance of deep water masses, by periods of enhanced continental runoff, or even by

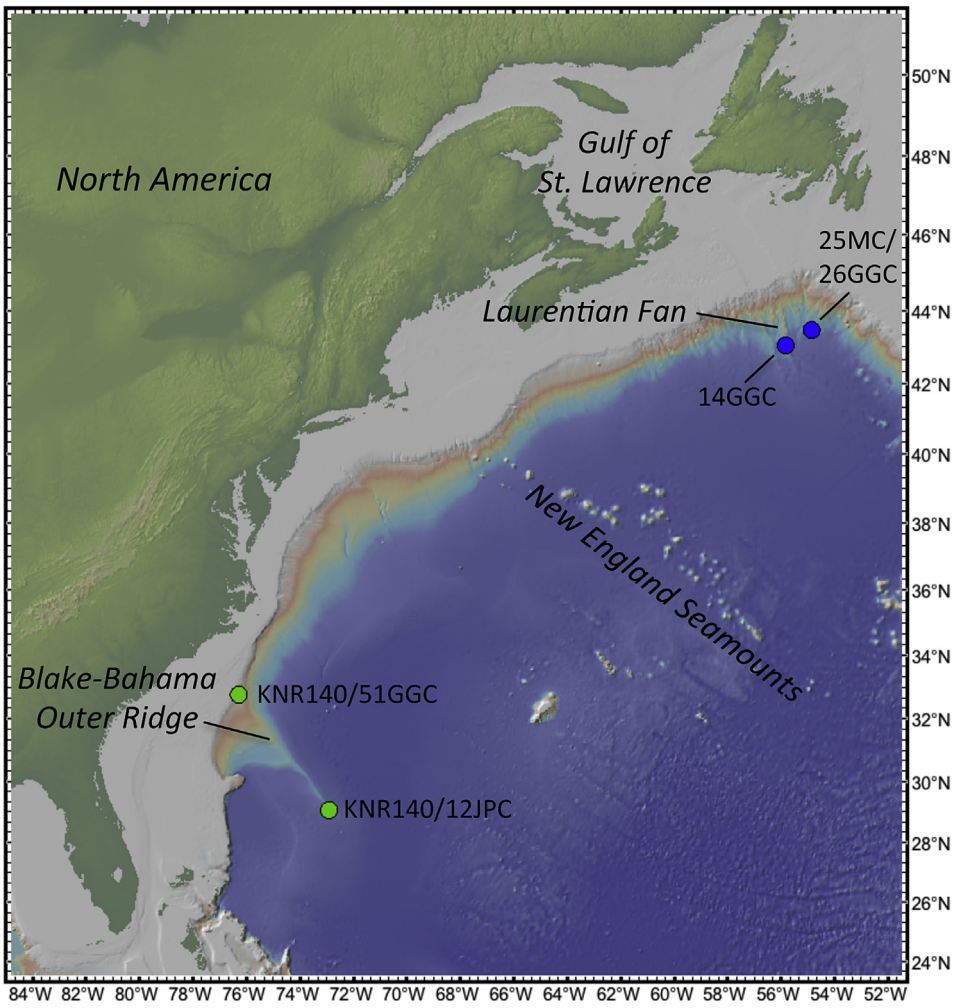

Fig. 1. Regional northwest Atlantic bathymetric map with core sites chosen for the Hf isotopic work along the Blake-Bahama Outer Ridge. Also shown are cores at the deeper Laurentian Fan outside the Gulf of St. Lawrence for comparison with the Pb isotopic records. Map was generated using GeoMapApp (http://www.geomapapp.org/) using the bathymetric configuration of Ryan et al. (2009).

changes in basal physicochemical conditions underneath the eastern Laurentide Ice Sheet.

2. Material and Methods

Two sediment cores spanning the past 26 ka recovered during KNR140 cruise along the Blake Ridge in the western North Atlantic were selected for Hf isotope analyses (Fig. 1). This pre-site survey of ODP Leg 172 aimed at coring a multitude of sites along the large sediment drift body. Late Pleistocene and Holocene sediments along the upper part of the Blake Ridge consist of nannofossil ooze and silty clay with variable proportions of biogenic and siliciclastic components. The carbonate content in the sequences of the upper part of the Blake Ridge varies between 34 and 67% (Keigwin et al., 1997). The deepest sections of the Blake Ridge are dominated by alternating carbonate-rich and carbonate-poor units, ranging from nannofossil-ooze in the most carbonate-rich sections (20–55% carbonate) to essentially terrigenous clay (2–15% carbonate) (Keigwin et al., 1997).

Cores KNR140/51GGC from 1790 m water depth and KNR140/12JPC from 4250 m depth were selected to reconstruct the seawater Hf isotope evolution in the intermediate and deep western North Atlantic as recorded by authigenic sedimentary Fe–Mn oxyhydroxides. Sedimentation rates at shallow site 51GGC ranged from ca 6 cm/ka during the LGM to approximately 25 cm/ka during the late Holocene (Gutjahr et al., 2008). At Core 12JPC, the section preceding 20 ka experienced sedimentation rates close to 72 cm/ka, average sedimentation rates of 22 cm/ka during the deglaciation, and lowest sedimentation rates during the Holocene (~4.7 to 7.8 cm/ka) (Table 1). The sections with the high sedimentation rates were a consequence of sediment focussing in both cores (Gutjahr et al., 2008).

The method to extract the seawater-derived Hf isotope signal through sequential reductive leaching followed that described in Gutjahr et al. (2007) and later applied by Chen et al. (2012). Samples were first decarbonated using a Na acetate buffer, followed by a three-hour leach in a 1M $MgCl_2$ solution, triple rinsed in deionised water and finally a three-hour reductive leach using a mixture of 0.05M hydroxylamine hydrochloride, 15% acetic acid, buffered to pH 4 with NaOH. Analogous to thorium, Hf is a high field strength element that is highly particle-reactive. Therefore 0.03M Na-EDTA was admixed to the reductive leach solution as a complexing reagent to avoid re-adsorption of Hf leached during Fe–Mn oxyhydroxide dissolution. For a subset of nine samples from Cores 51GGC and 12JPC the corresponding detrital fraction was completely dissolved and analysed as well in order to monitor

Table 1
New and previously published radiocarbon ages for core KNR140/12JPC.

Source/new lab number	Sample material	Depth in core (cm)	Conventional radiocarbon age (years BP)	Error	Calibrated age (years BP)	Error	Sedimentation rate per interval (cm/ka)[a]
ETH# 41215	Mixed planktic foraminifera	40	4863	52	**5106**	115	7.83
Robinson et al. (2005)	Mixed benthic foraminifera	66	10,300	220	**10,575**	108	4.75
Keigwin (2004)	Mixed planktic foraminifera	79	10,950	55	**12,486**	81	6.80
ETH# 41214	Mixed planktic foraminifera	93	12,274	101	**13,701**	126	11.52
Keigwin (2004)	Mixed planktic foraminifera	231	17,300	95	**20,048**	18	21.74
ETH# 41213	Mixed planktic foraminifera	290	17,938	161	**20,872**	257	71.60

Note: All planktic conventional foraminifera ages have been asigned a local reservoir effect of 408 years irrespective of ages (cf. Robinson et al., 2005).
[a] Linearly interpolated sedimentation rate between age tie points above the sampled depth.

potential partial dissolution of the detrital fraction during the leaching procedure (see Gutjahr et al. (2007) for more detailed analytical procedures).

Elemental purification of Hf in the Fe–Mn oxyhydroxide and detrital fractions followed the method of Münker et al. (2001). The total procedural Hf blank of the Fe–Mn oxyhydroxide analyses was below 30 pg (below 0.3% of the total Hf concentrations of the samples) and below 20 pg for the detrital fraction in the sediment, and is hence considered negligible. Hafnium isotope analyses were conducted on a Nu Plasma MC-ICPMS at ETH Zürich. Measured Hf isotope compositions were normalised to a $^{179}Hf/^{177}Hf$ of 0.7325 to correct for instrumental mass bias. Mass interferences originating from remaining Yb, Lu and W on various Hf isotopes in the purified samples were monitored by measuring the intensities of ^{172}Yb, ^{175}Lu and ^{182}W during every Hf isotope measurement. Mass-bias corrected Hf isotope compositions were normalised to a $^{176}Hf/^{177}Hf$ of 0.282160 for the JMC475 standard (Nowell et al., 1998). The external reproducibility in the course of this study was ±0.49 ε_{Hf} for $^{176}Hf/^{177}Hf$ (2σ, $n = 61$) at total Hf ion currents between 4 and 11×10^{-11} A. Detailed results of the Hf isotope analyses can be found in Table 2. Several duplicate measurements were carried out to evaluate the reproducibility of the Hf isotope extraction during reductive leaching. In Table 2 and Figs. 3 and 4 the individual results are displayed. For the reconstruction of the Hf isotope evolution of Cores 51GGC and 12JPC in Figs. 5–8 the average Hf isotope composition of the duplicates for every sampled depth was used.

Hafnium concentrations and Al/Hf were measured on a sub-set of eight samples similar to the approach of Gutjahr et al. (2007) in the same samples to determine the distribution of Hf in the different sedimentary phases and to compare these with other trace metals (Table 3). In detail, two subsequent separate Fe–Mn oxyhydroxide leach fractions using the same leaching reagent that were allowed to react for 3 h and 24 h, respectively, and the residual detrital elemental concentrations were measured by ICP-OES and ICP-MS at the Geological Institute of the University of Kiel (Germany).

The timescale used for Core 51GGC is identical to the one described in Gutjahr et al. (2008) using the radiocarbon ages measured on planktic foraminifera in Keigwin (2004). For Core 12JPC, three new radiocarbon ages of planktonic foraminiferal shells were produced to better constrain the chronology in this dynamic sedimentation regime. Accelerator Mass Spectrometry (AMS) ^{14}C measurements were made at the Laboratory of Ion Beam Physics at the ETH Zürich. A gas ion source allowed the direct injection of CO_2 from the samples into the AMS thus enabling ^{14}C-analyses of ultra-small sample quantities (Wacker et al., 2013). Conventional radiocarbon ages were converted into calendar ages using a surface water reservoir age of 408 years (cf. Robinson et al., 2005) and by applying Oxcal 4.1 (Bronk Ramsey, 2009) on the basis of the INTCAL data set (Reimer et al., 2009). The three new, as well as the three previously published radiocarbon ages are shown in Table 1, together with the sedimentation rates calculated by linear interpolation between individual age tie points without further smoothing. Application of this refined stratigraphy leads to slightly younger ages for the late Holocene sections (max. ΔT is 1.31 ka at 5.11 ka) and slightly older ages for the deglacial section of the core (max. ΔT is 1.20 ka at 18.76 ka) than the ones published by Gutjahr et al. (2008, 2009).

3. Results

Our findings presented below are subdivided into two major sections. First, the element geochemical and isotopic results extracted from the authigenic Fe–Mn oxyhydroxide and detrital fractions are shown and compared. Thereafter, Hf isotope time series of past seawater obtained from the authigenic Fe–Mn oxyhydroxide fraction of the two sediment cores covering the Last Glacial–interglacial transition are discussed.

3.1. Elemental ratios

In Gutjahr et al. (2007), Al/Nd, Al/Pb and Al/Th were presented for two successive Fe–Mn oxyhydroxide leachate fractions using identical reductive leaching solutions, together with the respective elemental ratios of the coexisting detrital phase. The first Fe–Mn oxyhydroxide leach fraction is used for paleoceanographic reconstructions while the second leachate served as a 24-h "buffer" leach since the authigenic Fe–Mn oxyhydroxide phase is not quantitatively removed during the first three-hour leach stage at room temperature. Generally, Al/(Nd, Pb, Th) were lowest for the first Fe–Mn oxyhydroxide coating fractions after three hours of leaching, slightly elevated for a second aliquot extracted after another 24 h of reductive leaching, and orders of magnitude higher for the detrital fraction (Gutjahr et al., 2007). The compositional differences observed during these experiments reflect the enrichment of the trace metals Nd, Pb and Th in the Fe–Mn oxyhydroxide fraction relative to Al. This is the result of preferential incorporation (sorption and co-precipitation) of seawater- and pore water derived particle reactive trace metals in the authigenic Fe–Mn oxyhydroxides.

Investigating Al/Hf in the same successive leach fractions and the residue reveals a similar but less pronounced enrichment of Hf relative to Al, at least in the first extracted Fe–Mn oxyhydroxide phase. As observed for Al/(Nd, Pb, Th), the first Fe–Mn oxyhydroxide leach displays lower Al/Hf than the respective detrital fraction (average Al/Hf of ~990; Fig. 2, Table 3), whereas the Al/Hf of the second Fe–Mn oxyhydroxide leach is in the same range as of the detrital fraction (average Al/Hf of ~3000 and ~3200, respectively). The Al/Hf of the first leach fraction is similar to or even lower than average Pacific ferromanganese crust ratios with a mean Al/Hf of 1445 (dashed grey box in Fig. 2; Table 3) (Hein et al., 1999).

Table 2
Hf isotope compositions of all analysed Fe–Mn oxyhydroxide and detrital samples.

Depth in core (cm)	Calendar age (ka)	$^{176}Hf/^{177}Hf$ ± internal error (2σ)	ε_{Hf} ± applicable error (2σ)	$\triangle\varepsilon_{Hf}$[a]
Fe–Mn oxyhydroxide fractions				
KNR140, Core 12JCP, 4250 m (29°04.48' N, 72°53.90' W)				
20 cm	2.55	0.282815 ± 6	1.5 ± 0.50	
duplicate		0.282814 ± 7	1.5 ± 0.50	0.05
30 cm	3.83	0.282829 ± 6	2.0 ± 0.50	
50 cm	7.21	0.282777 ± 7	0.2 ± 0.50	
55 cm	8.26	0.282771 ± 7	0.0 ± 0.50	
duplicate		0.282780 ± 11	0.3 ± 0.50	−0.34
69 cm	11.02	0.282766 ± 5	−0.2 ± 0.50	
77 cm	12.19	0.282775 ± 6	0.1 ± 0.50	
85 cm	13.01	0.282788 ± 8	0.6 ± 0.50	
duplicate		0.282790 ± 9	0.6 ± 0.50	−0.05
102 cm	14.11	0.282840 ± 6	2.4 ± 0.50	
117 cm	14.80	0.282752 ± 7	−0.7 ± 0.50	
140 cm	15.86	0.282786 ± 5	0.5 ± 0.50	
156 cm	16.60	0.282822 ± 9	1.8 ± 0.50	
172 cm	17.33	0.282781 ± 6	0.3 ± 0.50	
193 cm	18.30	0.282752 ± 7	−0.7 ± 0.50	
203 cm	18.76	0.282764 ± 7	−0.3 ± 0.50	
220 cm	19.54	0.282727 ± 9	−1.6 ± 0.50	
233 cm	20.08	0.282697 ± 6	−2.6 ± 0.50	
duplicate		0.282671 ± 8	−3.6 ± 0.50	0.95
251 cm	20.33	0.282720 ± 6	−1.8 ± 0.50	
263 cm	20.49	0.282682 ± 15	−3.2 ± 0.54	
duplicate		0.282702 ± 9	−2.5 ± 0.50	−0.69
KNR140, Core 51GGC, 1790 m (32°47.04' N, 76°17.18' W)				
40 cm	1.59	0.282860 ± 10	3.1 ± 0.50	
duplicate		0.282815 ± 29	1.5 ± 1.03	1.59
60 cm	2.39	0.282872 ± 14	3.5 ± 0.50	
duplicate		0.282834 ± 30	2.2 ± 1.07	1.37
160 cm	6.36	0.282835 ± 11	2.2 ± 0.50	
duplicate		0.282863 ± 27	3.2 ± 0.95	−0.97
220 cm	8.75	0.282829 ± 10	2.0 ± 0.50	
260 cm	10.34	0.282799 ± 9	0.9 ± 0.50	
270 cm	10.73	0.282868 ± 14	3.4 ± 0.50	
290 cm	11.20	0.282876 ± 9	3.7 ± 0.50	
300 cm	12.06	0.282870 ± 9	3.5 ± 0.50	
duplicate		0.282825 ± 18	1.9 ± 0.64	1.57
310 cm	12.89	0.282930 ± 13	5.6 ± 0.50	
330 cm	13.01	0.282960 ± 15	6.6 ± 0.51	
duplicate		0.282888 ± 11	4.1 ± 0.50	2.55
350 cm	15.05	0.282939 ± 10	5.9 ± 0.50	
duplicate		0.282870 ± 9	3.5 ± 0.50	2.44
370 cm	17.16	0.282948 ± 10	6.2 ± 0.50	
duplicate		0.282850 ± 11	2.7 ± 0.50	3.49
371 cm	17.22	0.282930 ± 6	5.6 ± 0.50	
duplicate		0.282835 ± 11	2.2 ± 0.50	3.35
373 cm	17.35	0.282840 ± 7	2.4 ± 0.50	
378 cm	17.65	0.282867 ± 10	3.4 ± 0.50	
385 cm	21.36	0.282805 ± 10	1.2 ± 0.50	
390 cm	22.15	0.282797 ± 11	0.9 ± 0.50	
duplicate		0.282763 ± 13	−0.3 ± 0.50	1.19
395 cm	22.94	0.282774 ± 15	0.1 ± 0.54	
400 cm	23.73	0.282734 ± 8	−1.4 ± 0.50	
duplicate		0.282741 ± 15	−1.1 ± 0.54	−0.26
405 cm	24.52	0.282735 ± 7	−1.3 ± 0.50	
duplicate		0.282713 ± 16	−2.1 ± 0.56	0.79
412 cm	25.62	0.282765 ± 9	−0.3 ± 0.50	
422 cm	27.20	0.282911 ± 9	4.9 ± 0.50	
Detrital fraction				
KNR140, Core 12JCP, 4250 m				
55	11.20	0.282419 ± 7	−12.4 ± 0.50	
85	12.67	0.282462 ± 7	−10.8 ± 0.50	
263	20.05	0.282509 ± 6	−9.2 ± 0.50	
KNR140, Core 51GGC, 1790 m				
60	2.39	0.282447 ± 8	−11.4 ± 0.50	
270	10.73	0.282469 ± 7	−10.6 ± 0.50	
350	15.05	0.282395 ± 7	−13.2 ± 0.50	
390	22.15	0.282319 ± 8	−15.9 ± 0.50	
400	23.73	0.282314 ± 7	−16.1 ± 0.50	

[a] Delta ε_{Hf} refers to the difference between duplicate analyses.

The less pronounced difference in Al/Hf between the first leachate and the detrital fraction was expected given the very low concentrations of Hf in the second Fe–Mn oxyhydroxide leach fractions (Table 3). Hafnium concentrations in the first Fe–Mn oxyhydroxide leach fraction range from 24 to 100 ng per gram of leached bulk sediment, which is orders of magnitude lower than those of Nd and Pb in the same fractions (Table 3). This is also reflected in distinct Nd/Hf and Pb/Hf between the three different phases (Table 3). Hafnium is also depleted in the Fe–Mn oxyhydroxide fraction relative to Nd and Pb when compared with the respective Nd/Hf and Pb/Hf in the detrital fraction, consistent with Hf/Nd and Hf/Pb ratios of ferromanganese crusts (Hein et al., 1999). It is worth mentioning that the second Fe–Mn oxyhydroxide leach fraction contains lower [Hf] (between 47 and 85%) than the first leach fraction. In contrast, Al concentrations in the second leach fraction are between 1.2 and 4.4 times higher than in the first one. In other words, while trace amounts of Al were continuously transferred into solution during the second (24-h) leach the Hf release was significantly reduced relative to the first (three-hour) leach. In summary, these data support that the first leach is suitable to extract past seawater Hf isotope compositions from the sediments of our study.

3.2. Reproducibility of the leachate data and comparison between authigenic and detrital signal

Isotopically the authigenic Fe–Mn oxyhydroxide fraction is significantly more radiogenic than its detrital counterpart throughout (Fig. 3). The differences between two fractions vary between 6.3 ε_{Hf} units (12JPC-263 cm) and 17.9 ε_{Hf} units (51GGC-350 cm). For deep Core 12JPC the reproducibility between duplicates of the leachate data is always better than 0.7 ε_{Hf} (Fig. 3). Duplicates for shallower Core 51GGC did not reproduce as well. The majority of duplicate ε_{Hf} data of this core agree within 1.6 ε_{Hf} but there is a deglacial section, in which the reproducibility of the duplicates is poorer (highlighted box in Fig. 3) and in which the data differ by between 2.4 and 3.5 ε_{Hf} units. Despite this poorer reproducibility, the ε_{Hf} signatures in Core 51GGC also trend towards less radiogenic compositions in the LGM section analogous to the trend observed in Core 12JPC. Consequences with regard to the reliability of the Hf isotope signal extracted from Core 51GGC will be discussed in Section 4.1.

3.3. Authigenic Hf isotope variability over the last glacial–interglacial transition

The Hf isotope record of Core 12JPC only extends back to the latest LGM at ~20.5 ka. Extracted authigenic Hf isotope signatures in both cores show a general trend from unradiogenic compositions during or before the LGM to significantly more radiogenic compositions afterwards (Fig. 4a and b). Least radiogenic (lowest) ε_{Hf} signatures in Core 12JPC were recorded at 20.1 ka (average glacial $\varepsilon_{Hf} = -3.1$) (Fig. 4a), while the least radiogenic data in Core 51GGC were already recorded at 24.5 ka (average glacial $\varepsilon_{Hf} = -1.7$) (Fig. 4b), a time interval not covered by Core 12JPC. Hence ε_{Hf} already increased during the LGM in Core 51GGC.

The early change in ε_{Hf} towards more radiogenic authigenic compositions during or immediately following the LGM (26.5–19.5 ka) (Clark et al., 2009) (Fig. 4a and b) highlights that the authigenic Hf isotope evolution followed a significantly different phasing compared with the authigenic Pb isotope evolution in both cores (Fig. 4a/c and b/d) (Gutjahr et al., 2009). The Hf isotope record is essentially anti-correlated with the Nd isotope record of site 51GGC (Fig. 4b and f) and at least decoupled from the Nd isotope record of Site 12JPC (Fig. 4a and e) (Gutjahr et al., 2008).

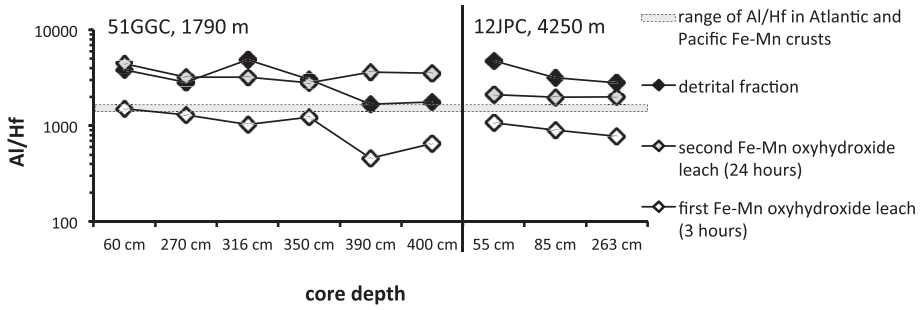

Fig. 2. Aluminium/hafnium elemental ratios of two successive (3-h and 24-h) reductive leach fractions and the corresponding detrital fraction of Blake Ridge sediments. Elemental ratios for the first extracted Fe–Mn oxyhydroxide fraction that was used for the isotope analyses (white diamonds) average to 989 and are lower than average hydrogenetic ferromanganese crusts in the equatorial Central and South Pacific (Hein et al., 1999) yielding a mean Al/Hf of 1445 (grey horizontal dashed box; see also Table 3). Elemental ratios of the second leach, however, fall in the range of Al/Hf of the detrital fractions. Note the logarithmic *y*-axis. The individual Al/Hf for samples presented here are also displayed in Table 3.

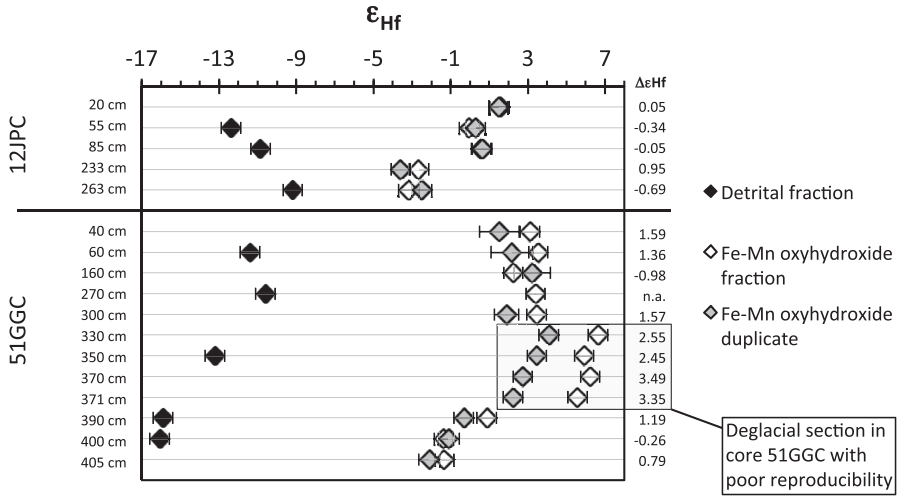

Fig. 3. Range and reproducibility of ε_{Hf} for Blake Ridge Fe–Mn oxyhydroxide fraction replicates as well as samples for which the detrital fraction was also isotopically analysed, arranged per depth in core. Most authigenic duplicates reproduced within analytical error. Deglacial section in Core 51GGC with relatively poor reproducibility is highlighted. $\Delta\varepsilon_{Hf}$ refers to the difference in absolute ε_{Hf} between duplicates. Results are also displayed in Table 2.

3.4. Neodymium–hafnium isotope trends

Consistent with ferromanganese crust and present-day dissolved seawater compositions, the combined ε_{Hf} and ε_{Nd} data of the Fe–Mn oxyhydroxide fractions extracted from the Blake Ridge sediments plot on the seawater array (Fig. 5). For deep Core 12JPC there is reasonable agreement with the range of isotope compositions of ferromanganese crusts ALV539 and BM1969.05 (Burton et al., 1999; Piotrowski et al., 2000) from the western North Atlantic spanning the last 3 Myr (Fig. 5c). However, the Fe–Mn oxyhydroxide fractions of the two different sediment cores define trends that are distinct from each other and from the NW Atlantic ferromanganese crust data. For Core 51GGC, the inverse correlation between ε_{Hf} and ε_{Nd} mentioned above (Fig. 4b and f) is evident (Fig. 5b). In fact, the isotopic variability displayed by the Fe–Mn oxyhydroxide fraction data of this core defines a trend almost perpendicular to the slope of the seawater array. In Core 12JPC, several Holocene samples are essentially identical with late Pleistocene compositions of crust ALV539 (Burton et al., 1999; Piotrowski et al., 2000), while deglacial and LGM samples in 12JPC are more radiogenic in ε_{Nd} and partly significantly less radiogenic in ε_{Hf}. In both cores the data closest to the terrestrial array correspond to the LGM sections (Fig. 5b and c) yet still have more radiogenic ε_{Hf} than crustal rocks with the same ε_{Nd} (Fig. 5a).

4. Discussion

Extracting a pure seawater-derived Hf isotope signal from deep marine sediments is not trivial and to date only one recent study presented a sediment-derived paleo-seawater Hf isotope record (Chen et al., 2012). Most authigenic Fe–Mn oxyhydroxide-derived Hf isotope results presented here appear reliable based on:

(1) low Hf concentrations suggesting detrital phases were not leached
(2) the associated low Al/Hf
(3) good to excellent reproducibility for most samples apart from the deglacial section in 51GGC
(4) Hf isotopic compositions that are much more radiogenic than corresponding detrital fractions
(5) good agreement with the well established Nd–Hf isotope "seawater array"; and
(6) with corresponding water column and ferromanganese crust isotope data

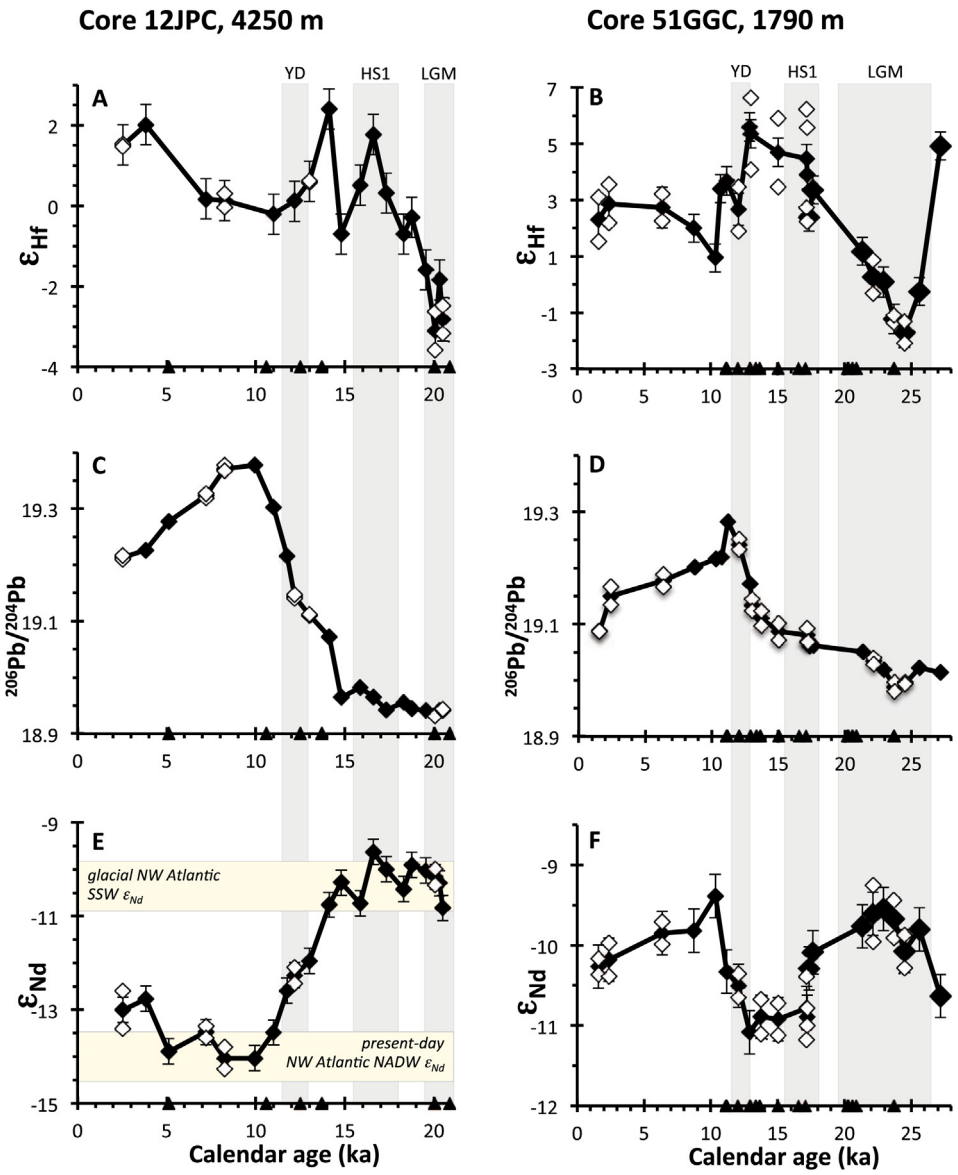

Fig. 4. Authigenic Fe–Mn oxyhydroxide-derived ε_{Hf}, $^{206}Pb/^{204}Pb$ and ε_{Nd} evolution in Cores 12JPC in 4250 m water depth and 51GGC in 1790 m water depth over the last glacial–interglacial transition. In levels for which replicates were obtained the individual results are plotted as white diamonds. Mean values for these depths were used to illustrate the individual isotopic trends. Note the generally excellent reproducibility for every isotope systems observed in Core 12JPC. The Pb and Nd isotopic records were published and discussed in Gutjahr et al. (2008, 2009). The Nd isotope record of site 12JPC (Fig. 4E) also highlights the composition of glacial SSW ε_{Nd} as observed in the NW Atlantic (Gutjahr et al., 2008; Roberts et al., 2010; Gutjahr and Lippold, 2011) and present-day NADW ε_{Nd} (Piepgras and Wasserburg, 1987). Triangles along age-axis mark sedimentary depths for which radiocarbon ages from planktic foraminifera are available (Keigwin, 2004; Robinson et al., 2005; as well as new ages shown in Table 1). YD: Younger Dryas, HS1: Heinrich Stadial 1, LGM: Last Glacial Maximum.

However, some of the data of intermediate depth Core 51GGC are less reproducible so before drawing paleoclimatic conclusions we first revisit some of the above elemental and isotopic properties of the chemically extracted phases and discuss these data in more detail to assess which data reflect an undisturbed seawater origin.

4.1. Integrity of the leached Hf isotope signal

Only trace amounts of Hf have been released during reductive leaching (Table 3). On average 54 ng Hf per gram of leached bulk sediment were extracted. Hence, compared with Nd and Pb that are both highly enriched in the Fe–Mn oxyhydroxide fraction (Table 3; Gutjahr et al., 2007), Hf is depleted in this phase. On the one hand the observation of such low Hf concentrations in the extracted fraction is encouraging since significant partial dissolution of the detrital fraction should lead to higher Hf concentrations. On the other hand this makes the Fe–Mn oxyhydroxide leachate signal more susceptible to contributions from partial dissolution of the detrital fraction despite that Hf is not highly concentrated in most detrital minerals.

Leachate element to aluminium ratios (e.g., Al/Hf; Fig. 2; Table 3) provide a good first-order estimate of potential contributions from the aluminosilicate fraction. Authigenic Fe–Mn oxyhydroxides are expected to contain little Al compared with the corresponding detrital phases. Sequential leaching of hydrogenetic Pacific ferromanganese crusts showed that they contain little Al from aluminosilicates but do contain a leachable Al phase most likely consisting of seawater-derived Al hydroxides (Koschinsky and

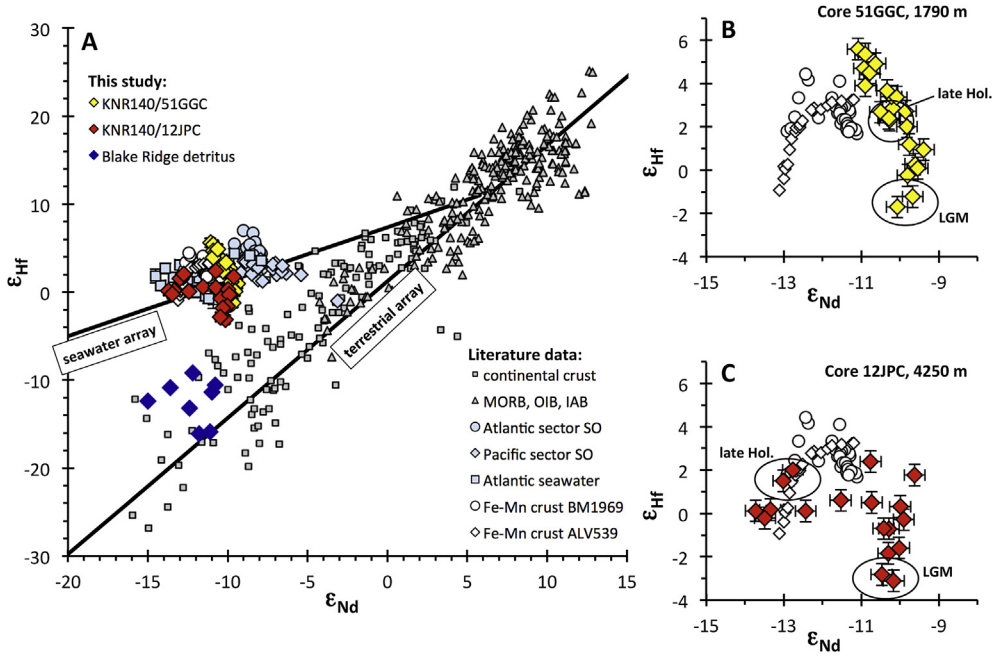

Fig. 5. **(A)** Hafnium–neodymium isotope systematics in extracted Fe–Mn oxyhydroxide fractions and detrital fraction from Blake Ridge sediments compared with published compositions of crustal and mantle rocks (Vervoort et al., 1999), hydrogenetic NW Atlantic Fe–Mn crusts (Lee et al., 1998; Piotrowski et al., 2000), as well as direct seawater measurements from the Atlantic (Rickli et al., 2009), Atlantic sector of the SO (Stichel et al., 2012a), the Pacific (Zimmermann et al., 2009b) and the Pacific sector of the SO (Rickli et al., 2014). Seawater- and terrestrial array systematics taken from Albarède et al. (1998) and Vervoort et al. (2011). **(B)** and **(C)** illustrate individual Fe–Mn oxyhydroxide fraction compositions in Cores 51GGC and 12JPC at expanded scale. Also plotted are the ferromanganese crust compositions of ALV539 (white diamonds) (Lee et al., 1998) and BM1969.05 (white circles) (Piotrowski et al., 2000), covering compositions of the past 3 Myr.

Halbach, 1995). Hence, if comparable to mineral phase associations in hydrogenetic Fe–Mn crusts, sedimentary authigenic marine Fe–Mn oxyhydroxides should contain at least trace amounts of leachable seawater-derived Al. Only 12–98 μg of Al per gram of leached sediment was extracted in the first reductive leach fraction (Table 3), suggesting that the bulk of this signal is authigenic in origin. Together with generally minute extracted Hf concentrations in the same fraction the observation of even lower leachate Al/Hf than reported for average Pacific ferromanganese crusts (Fig. 2) (Hein et al., 1999) is consistent with the conclusion that the only Hf pool significantly tapped during reductive leaching was authigenic and originated from seawater.

Besides low Al/Hf in the first Fe–Mn oxyhydroxide leach fraction, the extracted Hf isotope signal is also clearly distinct from the detrital signal (Figs. 3 and 5). While encouraging and in agreement with two earlier studies that chemically extracted the Hf in the Fe–Mn oxyhydroxide fraction from marine sediments (Bayon et al., 2009; Chen et al., 2012), this observation alone is not a proof of seawater-origin. As mentioned above, bulk continental and mantle rock ε_{Nd} and ε_{Hf} are well correlated, defining the terrestrial array (Vervoort et al., 1999). Hydrogenetic seawater precipitates such as ferromanganese crusts (Albarède et al., 1998; Piotrowski et al., 2000; David et al., 2001; van de Flierdt et al., 2004) or seawater signatures themselves (Godfrey et al., 2009; Rickli et al., 2009; Zimmermann et al., 2009b; Stichel et al., 2012a; Rickli et al., 2014) almost always have elevated ε_{Hf} for a given ε_{Nd} falling on the seawater array (Fig. 5a). Conversely, combined marine sedimentary ε_{Nd} and ε_{Hf} compositions can also deviate from the terrestrial array, induced by continental weathering and mineral and grain size sorting during transport to the oceans (Patchett et al., 1984; Vervoort et al., 2011; Garçon et al., 2013). The latter authors consistently reported relatively radiogenic Hf isotope compositions of hydrogeneous and terrigenous clays for a given Nd isotope signature.

Realistically, if the detrital phase in Blake Ridge sediments had been attacked during reductive extraction of the Fe–Mn oxyhydroxide phase, the detrital Hf would have been released from relatively radiogenic clays and not from weathering-resistant zircons (Vervoort et al., 2011; Garçon et al., 2013) (i.e., representing the unradiogenic Hf end member of the aluminosilicate phase). In such a case the mixed extracted Hf isotope signal would be relatively radiogenic as evident from leaching experiments on different grain size fractions of Chinese terrestrial dust (Chen et al., 2013b). The reliability of the seawater origin of the extracted Hf isotope compositions of any sediment can therefore only be ultimately tested by directly comparing core-top leachate compositions to ambient seawater measurements, which in our case cannot be provided due to the absence of dissolved seawater data directly from the core sites. However, we note that using the same reductive leaching approach, Chen et al. (2012) succeeded in extracting a deep water Hf isotope composition even from Arctic sediments that exclusively consist of silty clays (Moran et al., 2006). Furthermore, the closest published Hf isotope data from deep-water sampling stations available to the east of the Blake Ridge in the central North Atlantic match late Holocene Blake Ridge Fe–Mn oxyhydroxide compositions remarkably well. While the youngest sample in Core 12JPC has an ε_{Hf} of 1.5 ± 0.5, the average deepwater composition in the central North Atlantic varies between 0.27 and 1.76 ε_{Hf} (Godfrey et al., 2009).

Additional support for the reliability of the extracted authigenic Hf isotope signal is provided by the reproducibility of replicate measurements of sediment samples that separately underwent the complete chemical extraction procedure. In total 16 full replicates were processed in the course of this study (Table 2; Figs. 3 and 4). Essentially all replicates in Core 12JPC reproduced within error, while in 51GGC only depths covering the LGM and Holocene sections reproduced satisfactorily. In contrast, the replicates of the samples from the deglacial section of Core 51GGC reproduced

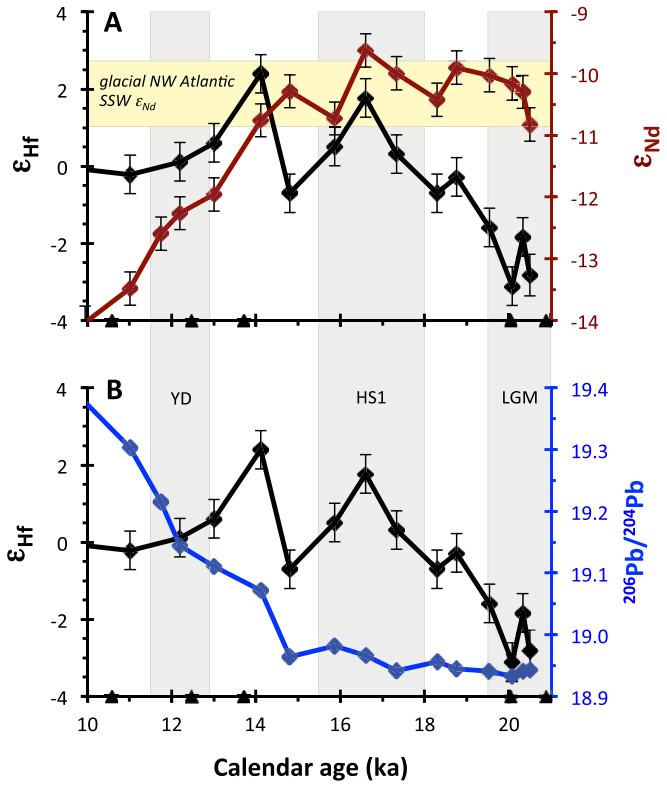

Fig. 6. Late-LGM and deglacial deep water Hf isotopic evolution at the Blake Ridge as recorded in Core 12JPC (4250 m), compared with **(A)** the corresponding mean Nd isotopic evolution shown in brown and **(B)** the $^{206}Pb/^{204}Pb$ evolution shown in blue. For samples in core for which replicates were produced (see Fig. 4) only the mean compositions per sampled depth are shown. Black triangles mark radiocarbon age tie points. YD: Younger Dryas, HS1: Heinrich Stadial 1, LGM: Last Glacial Maximum. Glacial NW Atlantic Southern Source Water ε_{Nd} is based on data from Gutjahr et al. (2008), Roberts et al. (2010) and Gutjahr and Lippold (2011). (For interpretation of the references to colour in this figure legend, the reader is referred to the web version of this article.)

rather poorly and partially yielded comparatively radiogenic ε_{Hf} which cast doubt on their reliability.

In summary, no entirely unambiguous proof for a pure hydrogenetic origin of the Hf in the Fe–Mn oxyhydroxide fractions can be offered in the context of our study. However, because of (i) the good reproducibility of many Hf samples (Fig. 4a), (ii) the good agreement with ferromanganese crust Al/Hf (Fig. 3), (iii) the earlier observed excellent match between central Arctic deep water and core top sediment leachate ε_{Hf} compositions reported by Chen et al. (2012) using the same extraction method and (iv) the good match between the closest deepwater sampling stations (Godfrey et al., 2009) and deep Blake Ridge leachates, we conclude that at least for Core 12JPC Fe–Mn oxyhydroxide-derived ε_{Hf} signatures represent ambient bottom water compositions. Conversely, owing to the poor reproducibility of some deglacial samples in Core 51GGC and slightly elevated Holocene ε_{Hf} compared with nearby seawater data (Godfrey et al., 2009), the Hf isotope record from this intermediate water site is only considered to the extent that we note an overall increase from unradiogenic ε_{Hf} during the LGM to more radiogenic compositions during the Holocene, as well as a change towards more radiogenic compositions initiated already during the LGM, which is not inconsistent with the deeper core site. The following paleoclimatic discussion and resulting implications will therefore largely focus on findings of Core 12JPC, which we consider to represent a fully reliable Hf isotope record of past deep water.

4.2. Early deglacial changes of North American continental inputs

Between 20.1 and 16.6 ka BP (i.e., within 3.5 ka) the deep water ε_{Hf} at site 12JPC became more radiogenic by 4.9 ε_{Hf} units from −3.1 to +1.8 while the ε_{Nd} at the same time remained virtually constant (Fig. 6a) changing only by 0.6 ε_{Nd} units from −10.2 to −9.6. The Nd isotope data obtained from the same and nearby cores provide clear evidence for the presence of deglacial Southern Source Water (SSW) at the sediment site throughout this interval (Gutjahr et al., 2008; Roberts et al., 2010; Gutjahr and Lippold, 2011), hence the early deglacial trend towards more radiogenic ε_{Hf} cannot be related to a change in deep water provenance and mixing but must have been controlled by changes in continental inputs, most likely from North America. To put this change in deep northwest Atlantic ε_{Hf} in perspective it is important to first consider the global Hf isotope variability in the modern oceans.

Compared with dissolved Nd that varies isotopically by more than 25 ε_{Nd} units in modern seawater (Lacan et al., 2012), the few existing published Hf isotopic data sets suggest a smaller range in seawater despite a larger range of Hf isotopic compositions in

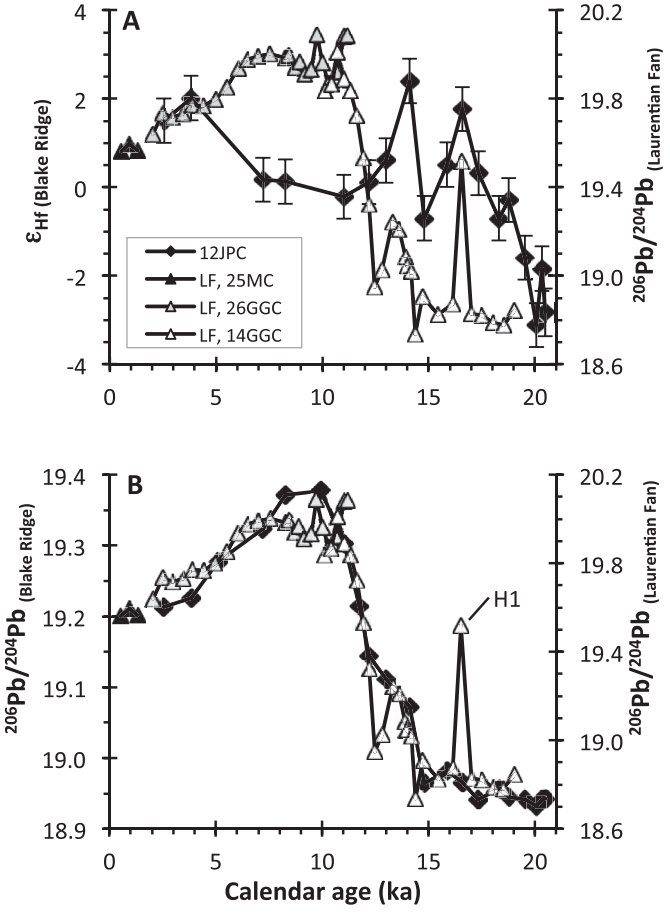

Fig. 7. Comparison of the deep Blake Ridge (Core 12JPC) and Laurentian Fan (Cores 25 MC, 26GGC, 14GGC) authigenic Hf and Pb isotopic records over the last glacial-interglacial transition. **(A)** Blake Ridge ε_{Hf} compared with Laurentian Fan $^{206}Pb/^{204}Pb$ evolution (Kurzweil et al., 2010), and **(B)** Blake Ridge authigenic $^{206}Pb/^{204}Pb$ (Gutjahr et al., 2009) compared with Laurentian Fan authigenic $^{206}Pb/^{204}Pb$ (Kurzweil et al., 2010). H1 refers to peak ice rafting conditions experienced during Heinrich event 1 at the Laurentian Fan site (Gil et al., 2010). Note the striking agreement in Pb isotopic changes seen between the two core sites that are >2000 km apart, both recording enhanced continental input initiating during the Bølling/Allerød interstadial, the Younger Dryas and transition to the Holocene. Stratigraphy from Laurentian core sites is from Keigwin et al. (2005). Chronology for the two sites were established independently and not matched (see methods for Blake Ridge stratigraphy).

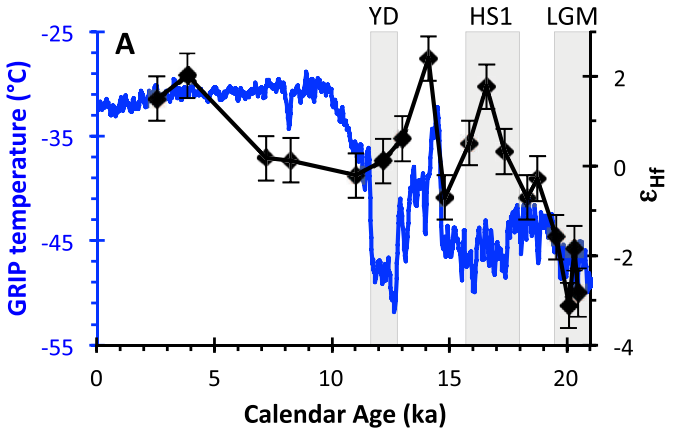

Fig. 8. Comparison of the Hf isotopic evolution observed at Blake Ridge site 12JPC with ice core-derived temperature records. **(A)** Core 12JPC ε_{Hf} plotted against reconstructed local temperatures at the GRIP site (Rasmussen et al., 2006; Rasmussen et al., 2008) using the temperature calibration of Cuffey and Clow (1997) ($T = 3.05^{*}\delta^{18}O+75.5$). Greenland temperatures have been smoothed using a five-point running average. Timing of the (i) LGM as defined in Clark et al. (2009) and (ii) HS1 from Barker et al. (2009).

crustal rocks from ε_{Hf} as low as −27 to values as radiogenic as +25 (Vervoort et al., 1999) (see also Fig. 5). Reported surface water ε_{Hf} vary from values of −5.7 ± 0.7 in 50 m water depth in the central North Atlantic (Godfrey et al., 2009) to compositions as high as +10.5 ± 0.8 in surface waters close to the Canary Islands (Rickli et al., 2010). However, the majority of the remaining surface and deep water ε_{Hf} data define a distinctly smaller range (Rickli et al., 2009; Zimmermann et al., 2009a, 2009b; Stichel et al., 2012a; Stichel et al., 2012b; Rickli et al., 2014). In seawater below 1000 m water depth the ε_{Hf} variability is diminished further. It is as low as −2.1 ± 0.85 at 1000 m in the Labrador Sea (Rickli et al., 2009) while the most radiogenic compositions are observed in the deep North Pacific (ε_{Hf} = 8.6 ± 1.6 in 5000 m) (Zimmermann et al., 2009b). Most deep water ε_{Hf} values reported to date show a narrow range from −1 to +6 (Godfrey et al., 2009; Rickli et al., 2009; Zimmermann et al., 2009a, 2009b; Stichel et al., 2012a; Rickli et al., 2014), with the exception of the restricted basin of the Baltic Sea (Chen et al., 2013a). Given the large lithological range of crustal ε_{Hf} mentioned above (Vervoort et al., 1999) this small variability highlights the importance of incongruent weathering and thus isotopically relatively homogenous continental input of Hf into the oceans (Rickli et al., 2010). In other words, the diminished Hf isotopic variability in seawater today compared with the Nd isotopic range in seawater indeed seems to be largely controlled by the inaccessibility of zircon-derived unradiogenic Hf to continental runoff (cf., Patchett et al., 1984) resulting in an isotopically much less heterogenous dissolved Hf runoff flux than that of Nd. Certainly other major and minor mineral phases on the continents also release isotopically variable Hf (Bayon et al., 2006) yet the zircon-free portion of continental crust is bound to release a significantly less variable Hf isotope signal than bulk continental crust (van de Flierdt et al., 2007). As an example, dissolved ε_{Hf} in the Pacific sector of the Southern Ocean adjacent to Mesozoic sequences of West Antarctica (Rickli et al., 2014) is within error indistinguishable from that of the Atlantic sector of the Southern Ocean located next to old cratonic sequences of East Antarctica (Stichel et al., 2012a).

Below we compare the behaviour of the Pb and Hf isotope systems since both weather incongruently, are partially controlled by the same accessory mineral phases (Bayon et al., 2006), and both have been shown to respond to climate-driven physical and chemical weathering trends. The ε_{Hf} recorded in 4250 m water depth at the deep Blake Ridge during the LGM (mean $\varepsilon_{Hf} = -3.1$) is less radiogenic than any reported modern open ocean deep-water composition and changed towards more typical deep Atlantic ε_{Hf} signatures immediately after the LGM (Fig. 6). In contrast to this early deglacial increase in ε_{Hf}, the authigenic Fe–Mn oxyhydroxide-derived Pb isotope composition derived from the same core does not change until 6 ka later (~14.1 ka) (Fig. 6b). The Blake Ridge deep water Pb isotope record (Fig. 6b) was mainly controlled by the presence or absence of significant continental runoff from nearby North America (Gutjahr et al., 2009; Kurzweil et al., 2010). Both the Blake Ridge and the deeper Laurentian Fan core sites further north (Fig. 1) recorded late deglacial changes in runoff that only started during the Bølling/Allerød interstadial. The data of the two core sites impressively demonstrate the difference in distances of the input sources between the core sites with regard to these changing continental Pb inputs, as documented by the strikingly similar patterns and timings of change at the two sites albeit at significantly different amplitudes in Pb isotopic excursions (Fig. 7b). Note that the stratigraphies of the two sampling sites were established

Table 3
Al, Nd, Hf and Pb concentrations of ferromanganese crusts and sediment fractions.

	Al (mg/g)[a,b]	Hf (ppm)	Nd (ppm)	Pb (ppm)	Al/Hf	Nd/Hf	Pb/Hf
Central Equatorial Pacific[a]							
Marshall Is.	11.9	8.4	170	1799	1417	20	214
Johnston I.	14.2	10.5	210	1871	1352	20	178
South Pacific[a]	15.8	10.1	226	741	1567	22	73
				Average:	**1445**	**21**	**155**
THIS STUDY	Al(μg/g)[c]	Hf (μg/g)[c]	Nd (μg/g)[c]	Pb (μg/g)[c]	Al/Hf	Nd/Hf	Pb/Hf
First Fe–Mn oxyhydroxide leach (3 h)							
51GGC – 60 cm	36.1	0.024	3.52	1.37	1501	146	57
51GGC – 270 cm	49.0	0.038	4.95	2.18	1292	130	58
51GGC – 316 cm	24.7	0.024	2.50	1.14	1034	104	48
51GGC – 350 cm	50.4	0.041	3.89	2.63	1228	95	64
51GGC – 390 cm	11.9	0.026	2.31	1.10	459	89	42
51GGC – 400 cm	31.0	0.048	2.64	1.79	649	55	37
12JPC – 55 cm	97.7	0.091	4.19	6.35	1069	46	69
12JPC – 85 cm	82.2	0.091	4.68	6.12	899	51	67
12JPC – 263 cm	77.0	0.100	4.25	4.32	772	43	43
Average:	51	**0.054**	3.66	3.00	**989**	**84**	**54**
Second Fe–Mn oxyhydroxide leach (24 h)							
51GGC – 60 cm	85	0.019	1.56	0.74	4479	82	39
51GGC – 270 cm	103	0.032	2.90	1.53	3210	90	48
51GGC – 316 cm	48	0.015	0.81	0.97	3211	54	66
51GGC – 350 cm	87	0.031	2.12	2.16	2800	68	69
51GGC – 390 cm	53	0.015	0.61	0.39	3639	42	27
51GGC – 400 cm	80	0.023	0.75	0.43	3556	33	19
12JPC – 55 cm	116	0.055	1.83	2.09	2102	33	38
12JPC – 85 cm	122	0.061	2.41	2.78	1988	39	45
12JPC – 263 cm	146	0.073	2.70	2.21	1997	37	30
Average:	93	**0.036**	1.74	1.48	**2998**	**53**	**42**
Detrital fraction							
51GGC – 60 cm	7640	2.00	17.3	6.4	3818	8.6	3.2
51GGC – 270 cm	11054	3.87	26.6	11.9	2853	6.9	3.1
51GGC – 316 cm	6408	1.31	6.0	2.7	4896	4.6	2.1
51GGC – 350 cm	11375	3.75	27.4	9.4	3036	7.3	2.5
51GGC – 390 cm	6826	4.09	15.3	6.0	1668	3.7	1.5
51GGC – 400 cm	10190	5.72	24.1	8.0	1782	4.2	1.4
12JPC – 55 cm	14637	3.07	24.8	10.0	4770	8.1	3.3
12JPC – 85 cm	12956	4.07	40.8	12.8	3182	10.0	3.1
12JPC – 263 cm	13369	4.78	39.5	15.4	2797	8.3	3.2
Average	10495	**3.63**	24.6	9.2	**3200**	**6.9**	**2.6**

Al, Nd and Pb concentrations have been presented previously in Gutjahr et al. (2007).

[a] Literature data from Hein et al. (1999).

[b] Where possible Al concentrations were calculated on a loss-on-ignition free base.

[c] Concentration data given for sediments analysed in this study are normalised to mg per gram of raw sediment weighed in.

independently using calibrated planktic foraminiferal radiocarbon ages without any adjustments (Keigwin, 2004; Keigwin et al., 2005; and methods).

As a first order control, increasing temperature, precipitation and the availability of immature glacially eroded sediment in northeast America led to incongruent, radiogenic Pb isotopic runoff pulses during glacial terminations of the Pleistocene in general (Foster and Vance, 2006; Vance et al., 2009) and the last deglaciation in particular (Gutjahr et al., 2009; Kurzweil et al., 2010; Crocket et al., 2012). As mentioned earlier, this feature can be ascribed to the preferential weathering of uranium-rich accessory mineral phases that released a distinct radiogenic Pb isotopic runoff signal during incipient chemical weathering (Harlavan et al., 1998; Harlavan and Erel, 2002). In the case of northwest Atlantic deep water Pb isotope records, the size and geometry of the waning Laurentide Ice Sheet also exerted an important control. Until the Bølling/Allerød interstadial the major eastern runoff routes from interior North America were effectively still blocked by the Laurentide Ice Sheet (Licciardi et al., 1998; Shaw et al., 2006). Throughout most of the deglaciation the bulk northeast American glacial runoff was thus drained south towards the Gulf of Mexico via the Mississippi (Kennett and Shackleton, 1975; Leventer et al., 1982; Meckler et al., 2008; Sionneau et al., 2010). Runoff drainage patterns likely varied to some extent during the deglaciation (Licciardi et al., 1999; Clark et al., 2001) yet the real opening of the eastern route via the St Lawrence river only became evident and traceable by proxy data during the Younger Dryas (Lewis et al., 1994; Carlson et al., 2007; Kurzweil et al., 2010).

The Blake Ridge deep-water ε_{Hf} is clearly decoupled from the corresponding Pb isotope record (Fig. 6b). While Pb traced increasing chemical weathering and runoff rates during the latter part of the deglaciation, the Hf isotope records apparently responded most strongly to the decreasing influence of LGM-style glacial weathering intensity on the northeast American continent at the end of the LGM. Both Blake Ridge cores recorded least radiogenic ε_{Hf} during the LGM (Fig. 4a, b) but the data of both cores still plot significantly above the terrestrial array when directly comparing extracted Nd and Hf isotopic compositions (Fig. 5b, c). Release of some zircon-derived Hf to sub- or periglacial runoff represents the most feasible source leading to the unradiogenic compositions observed during the LGM (cf. Piotrowski et al., 2000; van de Flierdt et al., 2002), yet the net isotopic supply of Hf to the northwest Atlantic during the LGM was still incongruent. This prevailing but diminished glacial incongruence is not surprising since Hf even from powdered zircon material found in sub- or periglacial settings is likely not easily accessible for chemical weathering. Isotopic changes in Hf weathering and -runoff during the LGM are implied since the recorded deep NW Atlantic ε_{Hf} signature was less radiogenic during this interval, while the Nd isotope signal was more radiogenic. Usually the opposite would be expected by the coupled behaviour of Nd and Hf isotopes (Albarède et al., 1998) and reflects upon the fact that Hf derived from NE America was supplied into SSW occupying the deep North Atlantic during the LGM (Gutjahr et al., 2008; Roberts et al., 2010; Gutjahr and Lippold, 2011). An offset towards less radiogenic ε_{Hf} for a given ε_{Nd} plotting below the seawater array was also observed in Arctic authigenic Fe–Mn oxyhydroxide fractions spanning the last 14 Ma (Chen et al., 2012) and was interpreted to be controlled by continuously prevailing glacial weathering conditions on the high latitude Eurasian continent.

The early deglacial change in ε_{Hf} reflects significant reduction in the supply of the unradiogenic source component of dissolved and/or colloidal Hf to the northwest Atlantic, changing ε_{Hf} to compositions typically prevailing under interglacial weathering conditions. Hence deep NW Atlantic ε_{Hf} already recorded a diminishing influence of zircon-derived Hf while interior North America was still occupied by the LIS with an ice sheet of nearly LGM dimensions (Dyke and Prest, 1987; Marshall and Clark, 2002). In principle, this early change in ε_{Hf} could have been amplified or driven by increasingly incongruent Hf supply dominantly controlled by Lu-rich phases (Bayon et al., 2006; Rickli et al., 2010; Chen et al., 2011), thereby leading to the early deglacial excursion towards more radiogenic ε_{Hf}. Several REE-rich accessory mineral phases such as monazite, allanite and some apatites (characterised by highly radiogenic ε_{Hf} signatures), would also have high U and Th leading to the release of radiogenic Pb (Harlavan and Erel, 2002; Bayon et al., 2006). However, supply of Hf from Lu-rich accessory mineral phases is not supported by the corresponding variability in $^{206}Pb/^{204}Pb$ at the Blake Ridge and the deeper Laurentian Fan (Fig. 7) unless radiogenic Hf supply from Lu-rich mineral phases was overwhelmed by the concomitant relatively unradiogenic feldspar weathering signal (Bayon et al., 2012). Direct comparison of the Hf isotopic data with the respective $^{206}Pb/^{204}Pb$ in Core 12JPC illustrates that changes in ε_{Hf} were not reflected by changes in $^{206}Pb/^{204}Pb$. Core 51GGC may indicate some co-variation, yet the section in core showing this trend covers the deglacial interval, which is regarded as unreliable (see Section 4.1). Therefore, the lack of change in the corresponding Pb isotope records suggests that radiogenic Hf derived from weathering of Lu-rich mineral phases played at most a subordinate role in the late glacial change towards radiogenic ε_{Hf} unless the residence time of Hf in seawater was significantly longer compared with Pb allowing Hf delivery from a more distant continental source.

The key information, however, that is likely contained in the deep Blake Ridge Hf isotope evolution during and after the LGM relates to the proposed basal temperature evolution of the Laurentide Ice Sheet during and after the LGM. The base of the Laurentide Ice Sheet was at or near the pressure melting point in Arctic Canada during the LGM (Kleman and Hattestrand, 1999; Refsnider et al., 2012). Frozen- or thawed-bed conditions can occur underneath continental ice sheets depending on ice sheet thickness and climatic boundary conditions (Dahl-Jensen et al., 2003; Pattyn, 2010). On this basis Marshall and Clark (2002) modelled basal conditions during the Last Glacial cycle, concluding that the fraction of warm-based ice increased significantly immediately after the LGM. Such a transition in sub-glacial physicochemical weathering conditions was likely associated with changes in the sub- and periglacial Hf isotopic runoff signal. As a result, the switch to the more incongruent Hf isotope signal seen in deep northwest Atlantic seawater may ultimately document the transition from a dominantly cold-based to a warm-based Laurentide Ice Sheet configuration in the Atlantic sector of continental northeast America.

4.3. Late deglacial and Holocene divergence in Hf and Pb isotopic chemical weathering signatures

A further important difference in the deep northwest Atlantic isotopic evolution of Pb and Hf is apparent in the late deglacial and Holocene part of our records (Fig. 7a). Similar to the observations made for the early deglacial section above, the Hf and Pb isotopic trends observed in the post-Younger Dryas section of Core 12JPC do not co-vary, although both elements are released incongruently during chemical weathering. High chemical weathering rates in recently deglaciated regions of continental North America and Europe led to a well-defined runoff pulse carrying radiogenic Pb isotope signatures (Fig. 7b) at the transition to and during the Holocene (Gutjahr et al., 2009; Vance et al., 2009; Kurzweil et al., 2010; Crocket et al., 2012, 2013). This excursion was dominantly controlled by preferential weathering of accessory uranium-rich mineral phases that are also enriched in Lu (Bayon et al., 2006),

yet again no radiogenic Hf isotope excursion can be identified during this interval (Fig. 4a, b). Leaching experiments using dilute acids carried out on crushed igneous and sedimentary rocks (Bayon et al., 2006) as well as on powdered Mesozoic and Tertiary sediments (Rickli et al., 2013) were shown to release highly radiogenic Hf isotope compositions into solution in several cases. On the other hand, neither dissolved Hf from the Moselle basin rivers (Bayon et al., 2006), nor waters from four Swiss rivers draining a wide range of lithologies (Rickli et al., 2013) produced Hf isotopic values more radiogenic than modern seawater. Highly radiogenic Hf isotopic weathering signals have so far only been reported in two rivers. Chen et al. (2012) reported ε_{Hf} in the lower reaches of the Kalix River in Northern Sweden yielding an ε_{Hf} of +16 although this signal is not recognisably transferred into the Northern Baltic Sea. Even more extreme ε_{Hf} signatures of +24 and +128 were reported for the upper reaches of the Hudson River (Godfrey et al., 2007). Yet again, the nearest Fe–Mn crust-derived ε_{Hf} records from the NW Atlantic New England Seamounts (Lee et al., 1998; Piotrowski et al., 2000) bear no trace of a distinctly radiogenic Hudson River-sourced Hf isotope signal. Based on the lack of more radiogenic river water ε_{Hf} Rickli et al. (2013) concluded that the zircon-free portions of crustal rocks weather relatively congruently. This may not apply to all paleoenvironmental settings but the Hf isotopic trends seen along the deeper Blake Ridge equally suggest that the only clear climate-dependent chemical weathering effect apparent in the Blake Ridge record is the identification of enhanced Hf contributions from zircons via sub-glacial and/or periglacial weathering during the LGM. If a radiogenic Hf weathering spike was released from Lu-rich phases during any stage of our record then this signal was effectively outcompeted by the contributing unradiogenic phases, whether this was controlled by feldspar weathering alone or also contained contributions from ground zircons. Consequently, the most radiogenic signal observed in Core 12JPC over the past 20 ka was recorded at 14.1 ka, yielding an ε_{Hf} of only 2.4 ± 0.50.

4.4. Hafnium contributions from partial dissolution of IRD during Heinrich event 1?

A further detail in the combined deglacial Hf and Pb isotope records (Fig. 7a) deserves mentioning. The first "radiogenic" excursion in Core 12JPC is seen during Heinrich event 1 (H1) reaching an ε_{Hf} of +1.8 ± 0.5 (Fig. 8). The Laurentian Fan Core site 14GGC located to the north of the Blake Ridge studied in Kurzweil et al. (2010) is located within the North Atlantic IRD belt (Ruddiman, 1977; Heinrich, 1988). It witnessed elevated ice rafting and associated deposition of ice-rafted debris (IRD) during Heinrich event 1 (H1) (Gil et al., 2010). This peak in IRD deposition also led to a highly radiogenic authigenic Pb isotope signal supplied to the Laurentian Fan, interpreted to be controlled by the release of Fe–Mn oxyhydroxide-bound Pb from pre-formed terrestrial IRD-hosted Fe–Mn oxides (highlighted in Fig. 7b) (Kurzweil et al., 2010).

The Blake Ridge in the subtropical Atlantic is located outside the IRD belt (Vautravers et al., 2004), hence extraction of a terrestrial IRD-hosted Fe–Mn oxide-derived trace metal signal does not apply here. However, the first radiogenic spike in ε_{Hf} observed in Blake Ridge Core 12JPC matches peak-IRD deposition recorded in the Laurentian Fan Pb isotope record (Fig. 7a). It can be speculated that if IRD sinking through the water column further north was susceptible to partial dissolution similar to Saharan dust today, then it may have released relatively radiogenic Hf from pre-formed terrestrial Fe–Mn oxides to the ambient water column. Rickli et al. (2010) for example provided Hf solubility estimates for airborne Saharan dust in the NE Atlantic in the range of ~1–3% that was released incongruently relative to bulk dust compositions. If the deep water Hf concentration in the northwest Atlantic was elevated compared with surface water compositions then a traceable isotopic effect caused by partial IRD dissolution is unlikely since substantial quantities of IRD-derived dissolved Hf would be required. On the other hand, if deep water Hf concentrations were depleted similar to for example in the Labrador Sea (Rickli et al., 2009) or the Southern Ocean (Stichel et al., 2012a) today then partial contributions from sinking IRD to ambient deep water ε_{Hf} that was subsequently transferred to the Blake Ridge may be isotopically detectable. Based on the available data we cannot resolve whether the first radiogenic peak at ~16.8 ka was caused by partial dissolution of IRD further north during H1 and the suggested process is probably not efficient enough in transferring IRD-hosted Hf back into solution. Yet the coincidence of the Pb and Hf isotopic peaks in Fig. 7a is intriguing.

In contrast, if this first radiogenic excursion in ε_{Hf} during H1 was not driven by partial dissolution of IRD but reflects more radiogenic freshwater sourcing, then a third possibility arises in controlling the early deglacial change to more radiogenic ε_{Hf} besides diminishing zircon contributions from ground bulk rocks. Meltwater input to the North Atlantic during extreme ice rafting of H1 could have supplied somewhat radiogenic Hf to the North Atlantic without significant associated radiogenic Nd. Such a supply of radiogenic Hf is not entirely unfeasible given reports of extremely radiogenic dissolved river water ε_{Hf} of +24 and +128 in the upper reaches of the Hudson River today (Godfrey et al., 2007) yet this hypothesis needs further testing closer to the Laurentide Fan Site.

4.5. Potential effect of pre-formed oxides in intermediate depth Core 51GGC

Based on systematic ε_{Nd}-water depth relationships in conjunction with high rates of sediment focussing at Site 51GGC during the Holocene, Gutjahr et al. (2008) concluded that a significant proportion of pre-formed Fe–Mn oxyhydroxides were extracted at shallow and intermediate water depths along the Blake Ridge. Such an effect has also been observed at other near-continental marine sites close to major river mouths such as the Congo River (Bayon et al., 2004; Kraft et al., 2013). Pre-formed terrestrial or shallow marine Fe–Mn oxyhydroxides should also contain significant amounts of Hf. In Section 4.1 above, we decided not to put too much weight on the Hf isotopic record of core 51GGC due to the poor reproducibility of the deglacial section. However, we note that the absolute ε_{Nd} and ε_{Hf} values recorded in Core 51GGC for a given time are always more radiogenic than compositions seen in deep Core 12JPC. This could indeed be controlled by relatively local contributions to the authigenic ε_{Hf} signal analogously to the observed ε_{Nd}.

5. Conclusions

This first deep northwest Atlantic Hf isotope record of past seawater obtained from authigenic Fe–Mn oxyhydroxides of bulk sediments from the Blake Ridge provides new insights into the late glacial retreat of the Laurentide Ice Sheet and associated changes in North American chemical weathering and runoff composition during the transition from the Last Glacial Maximum to the Holocene. Authigenic Nd isotope compositions confirm that the late glacial changes in ε_{Hf} were not controlled by changes in deep water circulation and mixing. Further, the authigenic Pb isotopic composition in the same samples allows identification of intervals of enhanced continental runoff from North America during the late deglaciation that were clearly not associated with corresponding radiogenic Hf isotope excursions.

Not all extracted authigenic Hf isotope results appear reliable. While the general trends seen in shallow Core 51GGC (1790 m) appear reasonable, questions remain regarding the integrity of the

deglacial interval. On the other hand, authigenic ε_{Hf} of Core 12JPC in 4250 m water depth is remarkably reproducible, measured Al/Hf are below those of Pacific ferromanganese crusts indicative of the pure hydrogenetic origin of the extracted Hf isotope signal, and absolute ε_{Hf} for the youngest analysed sediments (2.55 ka) are in good agreement with the nearest direct deep seawater sampling station some distance away in the central North Atlantic today. This deep northwest Atlantic authigenic Hf isotope record is therefore considered to reliably reflect ambient seawater ε_{Hf} over the past 20 ka.

Although both Hf and Pb isotopes are known to be released incongruently during continental weathering, deep water ε_{Hf} signatures have been decoupled from the corresponding Pb isotope evolution recorded along the Blake Ridge during the deglaciation and the Holocene. We found no evidence that the marine Hf isotope budget in the northwest Atlantic was controlled by preferential weathering of Lu-rich accessory mineral phases after the termination of the LGM. The Hf isotope record rather seems to reflect a switch from more congruent weathering of the bulk continental crust during the LGM towards congruent weathering of the zircon-free fraction of continental crust during the deglaciation and the Holocene, in agreement with conclusions drawn by Rickli et al. (2013). Yet the ε_{Hf} trends seen at the deeper Blake Ridge may also be controlled by an overwhelming feldspar weathering signal after the LGM, masking a concomitant radiogenic Hf isotope weathering signal.

The deep-water ε_{Hf} signal at the Blake Ridge during the LGM was dominated by Hf inputs from nearby northeast American sources. Mean ε_{Hf} as low as −3.1 at 4250 m water depth during the LGM suggests that northern hemisphere glaciation indeed allowed more efficient mechanical weathering and erosion under glacial weathering conditions, also supplying a fraction of unradiogenic Hf derived from enhanced weathering of zircons to the Blake Ridge. Despite full glacial weathering conditions on continental northeast America the net supply of Hf was still incongruent as evidenced by coupled ε_{Nd}–ε_{Hf} systematics. The very early change to typical interglacial radiogenic ε_{Hf} signatures already during the LGM may have ultimately been controlled by the transition from a cold-based to a warm-based Laurentide Ice Sheet. This suggestion will need confirmation through future studies. If correct, the authigenic deep marine ε_{Hf} signal close to ice sheets may be a sensitive tool to reconstruct larger-scale basal continental ice sheet physics.

Acknowledgements

Funding for this project was provided by grant TH-12 02-2 of ETH Zürich. We acknowledge Felix Oberli, Claudine Stirling, Helen Williams, Sarah Woodland, Mark Rehkämper, Heiri Baur, Urs Menet, Donat Niederer, Bruno Rütsche and Andreas Süsli for their help in keeping the MC-ICPMS running smoothly and their support in the clean labs and with the computers. Tina van de Flierdt compiled and calibrated Hf isotope results for crusts ALV539 and BM1969.05. Dieter Garbe-Schönberg at the Geological Institute of the University of Kiel carried out the major and trace element ICP-AES and ICP-MS measurements. We thank two anonymous reviewers for their constructive comments that helped improving an earlier version of the manuscript. Claude Hillaire-Marcel is acknowledged for swift editorial handling.

References

Albarède, F., Simonetti, A., Vervoort, J.D., Blichert-Toft, J., Abouchami, W., 1998. A Hf–Nd isotopic correlation in ferromanganese nodules. Geophys. Res. Lett. 25, 3895–3898.

Barker, S., Diz, P., Vautravers, M.J., Pike, J., Knorr, G., Hall, I.R., Broecker, W.S., 2009. Interhemispheric Atlantic seesaw response during the last deglaciation. Nature 457, 1097–1102.

Basak, C., Martin, E.E., Kamenov, G.D., 2011. Seawater Pb isotopes extracted from Cenozoic marine sediments. Chem. Geol. 286, 94–108.

Bau, M., Koschinsky, A., 2006. Hafnium and neodymium isotopes in seawater and in ferromanganese crusts: the "element perspective". Earth Planet. Sci. Lett. 241, 952–961.

Bayon, G., Burton, K.W., Soulet, G., Vigier, N., Dennielou, B., Etoubleau, J., Ponzevera, E., German, C.R., Nesbitt, R.W., 2009. Hf and Nd isotopes in marine sediments: constraints on global silicate weathering. Earth Planet. Sci. Lett. 277, 318–326.

Bayon, G., Dennielou, B., Etoubleau, J., Ponzevera, E., Toucanne, S., Bermell, S., 2012. Intensifying weathering and land use in Iron age Central Africa. Science 335, 1219–1222.

Bayon, G., German, C.R., Boella, R.M., Milton, J.A., Taylor, R.N., Nesbitt, R.W., 2002. An improved method for extracting marine sediment fractions and its application to Sr and Nd isotopic analysis. Chem. Geol. 187, 179–199.

Bayon, G., German, C.R., Burton, K.W., Nesbitt, R.W., Rogers, N., 2004. Sedimentary Fe–Mn oxyhydroxides as paleoceanographic archives and the role of aeolian flux in regulating oceanic dissolved REE. Earth Planet. Sci. Lett. 224, 477–492.

Bayon, G., Vigier, N., Burton, K.W., Brenot, A., Carignan, J., Etoubleau, J., Chu, N.-C., 2006. The control of weathering processes on riverine and seawater hafnium isotope ratios. Geology 34, 433–436. http://dx.doi.org/10.1130/G22130.22131.

Blichert-Toft, J., Albarède, F., 1997. The Lu-Hf isotope geochemistry of chondrites and the evolution of the mantle-crust system. Earth Planet. Sci. Lett. 148, 243–258.

Bronk Ramsey, C., 2009. Bayesian analysis of radiocarbon dates. Radiocarbon 51, 337–360.

Bruland, K.W., Lohan, M.C., 2003. 6.02-controls of trace metals in seawater. In: Holland, H.D., Turekian, K.K. (Eds.), Treatise on Geochemistry. Pergamon, Oxford, pp. 23–47.

Burton, K.W., Lee, D.-C., Christensen, J.N., Halliday, A.N., Hein, J.R., 1999. Actual timing of neodymium isotopic variations recorded by Fe–Mn crusts in the western North Atlantic. Earth Planet. Sci. Lett. 171, 149–156.

Carlson, A.E., Clark, P.U., 2012. Ice sheet sources of sea level rise and freshwater discharge during the last deglaciation. Rev. Geophys. 50. Art. No.: RG4007.

Carlson, A.E., Clark, P.U., Haley, B.A., Klinkhammer, G.P., Simmons, K., Brook, E.J., Meissner, K.J., 2007. Geochemical proxies of North American freshwater routing during the Younger Dryas cold event. Proc. Natl. Acad. Sci. U. S. A. 104, 6556–6561.

Chen, T.-Y., Frank, M., Haley, B.A., Gutjahr, M., Spielhagen, R.F., 2012. Variations of North Atlantic inflow to the central Arctic Ocean over the last 14 million years inferred from hafnium and neodymium isotopes. Earth Planet. Sci. Lett. 353–354, 82–92.

Chen, T.-Y., Stumpf, R., Frank, M., Bełdowski, J., Staubwasser, M., 2013a. Contrasting geochemical cycling of hafnium and neodymium in the central Baltic Sea. Geochim. Cosmochim. Acta 123, 166–180.

Chen, T.Y., Li, G.J., Frank, M., Ling, H.F., 2013b. Hafnium isotope fractionation during continental weathering: implications for the generation of the seawater Nd–Hf isotope relationships. Geophys. Res. Lett. 40, 916–920.

Chen, T.Y., Ling, H.F., Frank, M., Zhao, K.D., Jiang, S.Y., 2011. Zircon effect alone insufficient to generate seawater Nd–Hf isotope relationships. Geochem. Geophys. Geosyst. 12. Art. No.: Q05003.

Clark, P.U., Dyke, A.S., Shakun, J.D., Carlson, A.E., Clark, J., Wohlfarth, B., Mitrovica, J.X., Hostetler, S.W., McCabe, A.M., 2009. The last glacial maximum. Science 325, 710–714.

Clark, P.U., Marshall, S.J., Clarke, G.K.C., Hostetler, S.W., Licciardi, J.M., Teller, J.T., 2001. Freshwater forcing of abrupt climate change during the last glaciation. Science 293, 283–287.

Clark, P.U., Pollard, D., 1998. Origin of the middle Pleistocene transition by ice sheet erosion of regolith. Paleoceanography 13, 1–9.

Crocket, K.C., Foster, G.L., Vance, D., Richards, D.A., Tranter, M., 2013. A Pb isotope tracer of ocean-ice sheet interaction: the record from the NE Atlantic during the Last Glacial/Interglacial cycle. Quat. Sci. Rev. 82, 133–144.

Crocket, K.C., Vance, D., Foster, G.L., Richards, D.A., Tranter, M., 2012. Continental weathering fluxes during the last glacial/interglacial cycle: insights from the marine sedimentary Pb isotope record at Orphan Knoll, NW Atlantic. Quat. Sci. Rev. 38, 89–99.

Cuffey, K.M., Clow, G.D., 1997. Temperature, accumulation, and ice sheet elevation in central Greenland through the last deglacial transition. J. Geophys. Res.-Oceans 102, 26383–26396.

Dahl-Jensen, D., Gundestrup, N., Gogineni, S.P., Miller, H., 2003. Basal melt at NorthGRIP modeled from borehole, ice-core and radio-echo sounder observations. In: Duval, P. (Ed.), Ann. Glaciol. vol 37, 207–212.

David, K., Frank, M., O'Nions, R.K., Belshaw, N.S., Arden, J.W., 2001. The Hf isotope composition of global seawater and the evolution of Hf isotopes in the deep Pacific Ocean from Fe–Mn crusts. Chem. Geol. 178, 23–42.

Dyke, A.S., Prest, V.K., 1987. Late Wisconsinan and Holocene history of the Laurentide ice sheet. Geogr. Phys. Quat. 41, 237–264.

Erel, Y., Harlavan, Y., Blum, J.D., 1994. Lead isotope systematics of granitoid weathering. Geochim. Cosmochim. Acta 58, 5299–5306.

Foster, G.L., Vance, D., 2006. Negligible glacial-interglacial variation in continental chemical weathering rates. Nature 444, 918–921.

Garçon, M., Chauvel, C., France-Lanord, C., Huyghe, P., Lavé, J., 2013. Continental sedimentary processes decouple Nd and Hf isotopes. Geochim. Cosmochim. Acta 121, 177–195.

Gil, I.M., Keigwin, L.D., Abrantes, F.G., 2010. Comparison of diatom records of the Heinrich event 1 in the Western North Atlantic. IOP Conf. Ser. Earth Environ. Sci. 9, 7 pp.
Godfrey, L.V., Field, M.P., Sherrell, R.M., 2008. Estuarine distributions of Zr, Hf, and Ag in the Hudson River and the implications for their continental and anthropogenic sources to seawater. Geochem. Geophys. Geosyst. 9. Art. No.: Q12007.
Godfrey, L.V., King, R.L., Zimmermann, B., Vervoort, J.D., Halliday, A., 2007. Extreme Hf isotope signals from basement weathering and its influence on the seawater Hf–Nd isotope array. Geochim. Et. Cosmochim. Acta 71, A334.
Godfrey, L.V., Lee, D.C., Sangrey, W.F., Halliday, A.N., Salters, V.J.M., Hein, J.R., White, W.M., 1997. The Hf isotopic composition of ferromanganese nodules and crusts and hydrothermal manganese deposits: implications for seawater Hf. Earth Planet. Sci. Lett. 151, 91–105.
Godfrey, L.V., Zimmermann, B., Lee, D.C., King, R.L., Vervoort, J.D., Sherrell, R.M., Halliday, A.N., 2009. Hafnium and neodymium isotope variations in NE Atlantic seawater. Geochem. Geophys. Geosyst. 10. Art. No.: Q08015.
Gutjahr, M., Frank, M., Halliday, A.N., Keigwin, L.D., 2009. Retreat of the Laurentide ice sheet tracked by the isotopic composition of Pb in western North Atlantic seawater during termination 1. Earth Planet. Sci. Lett. 286, 546–555.
Gutjahr, M., Frank, M., Stirling, C.H., Keigwin, L.D., Halliday, A.N., 2008. Tracing the Nd isotope evolution of North Atlantic deep and intermediate waters in the western North Atlantic since the last glacial maximum from blake Ridge sediments. Earth Planet. Sci. Lett. 266, 61–77.
Gutjahr, M., Frank, M., Stirling, C.H., Klemm, V., van de Flierdt, T., Halliday, A.N., 2007. Reliable extraction of a deepwater trace metal isotope signal from Fe–Mn oxyhydroxide coatings of marine sediments. Chem. Geol. 242, 351–370.
Gutjahr, M., Lippold, J., 2011. Early arrival of Southern Source Water in the deep North Atlantic prior to Heinrich event 2. Paleoceanography 26. Art. No.: PA2101.
Harlavan, Y., Erel, Y., 2002. The release of Pb and REE from granitoids by the dissolution of accessory phases. Geochim. Cosmochim. Acta 66, 837–848.
Harlavan, Y., Erel, Y., Blum, J.D., 1998. Systematic changes in lead isotopic composition with soil age in glacial granitic terrains. Geochim. Cosmochim. Acta 62, 33–46.
Hein, J.R., Koschinsky, A., Bau, M., Manheim, F.T., Kang, J.-K., Roberts, L., 1999. Cobalt-rich Ferromanganese Crusts in the Pacific. In: Cronan, D.S. (Ed.), Handbook of Marine Mineral Deposits. CRC Press, pp. 239–279.
Heinrich, H., 1988. Origin and consequences of cyclic ice rafting in the Northeast Atlantic Ocean during the past 130,000 years. Quat. Res. 29, 142–152.
Jacobsen, S.B., Wasserburg, G.J., 1980. Sm-Nd Isotopic evolution of chondrites. Earth Planet. Sci. Lett. 50, 139–155.
Keigwin, L.D., 2004. Radiocarbon and stable isotope constraints on Last Glacial Maximum and Younger Dryas ventilation in the western North Atlantic. Paleoceanography 19. Art. No.: PA4012.
Keigwin, L.D., Rio, D., Acton, G.D., 1997. Northwest Atlantic sediment drifts. In: Graber, K.K. (Ed.), Ocean Drilling Program, Leg 172 Preliminary Report.
Keigwin, L.D., Sachs, J.P., Rosenthal, Y., Boyle, E.A., 2005. The 8200 year B.P. event in the slope water system, western subpolar North Atlantic. Paleoceanography 20. Art. No.: PA2003.
Kennett, J.P., Shackleton, N.J., 1975. Laurentide ice sheet meltwater recorded in Gulf of Mexico deep-sea cores. Science 188, 147–150.
Kleman, J., Hattestrand, C., 1999. Frozen-bed Fennoscandian and Laurentide ice sheets during the Last Glacial Maximum. Nature 402, 63–66.
Koschinsky, A., Halbach, P., 1995. Sequential leaching of marine ferromanganese precipitates: genetic implications. Geochim. Cosmochim. Acta 59, 5113–5132.
Kraft, S., Frank, M., Hathorne, E.C., Weldeab, S., 2013. Assessment of seawater Nd isotope signatures extracted from foraminiferal shells and authigenic phases of Gulf of Guinea sediments. Geochim. Cosmochim. Acta 121, 414–435.
Kurzweil, F., Gutjahr, M., Vance, D., Keigwin, L., 2010. Authigenic Pb isotopes from the Laurentian Fan: changes in chemical weathering and patterns of North American freshwater runoff during the last deglaciation. Earth Planet. Sci. Lett. 299, 458–465.
Lacan, F., Tachikawa, K., Jeandel, C., 2012. Neodymium isotopic composition of the oceans: a compilation of seawater data. Chem. Geol. 300–301, 177–184.
Lee, D.C., Halliday, A.N., Christensen, J.N., Burton, K.W., Hein, J.R., Godfrey, L.V., 1998. High resolution Hf isotope stratigraphy of Fe-Mn crusts. In: American Geophysical Union Fall Meeting Conference Abstract.
Leventer, A., Williams, D.F., Kennett, J.P., 1982. Dynamics of the Laurentide ice sheet during the last deglaciation: evidence from the Gulf of Mexico. Earth Planet. Sci. Lett. 59, 11–17.
Lewis, C.F.M., Moore, T.C., Rea, D.K., Dettman, D.L., Smith, A.M., Mayer, L.A., 1994. Lakes of the Huron basin - their record of runoff from the Laurentide ice-sheet. Quat. Sci. Rev. 13, 891–922.
Licciardi, J.M., Clark, P.U., Jenson, J.W., Macayeal, D.R., 1998. Deglaciation of a soft-bedded Laurentide Ice Sheet. Quat. Sci. Rev. 17, 427–448.
Licciardi, J.M., Teller, J.T., Clark, P.U., 1999. Freshwater routing by the Laurentide ice sheet during the last deglaciation. In: Clark, P.U., Webb, R.S., Keigwin, L.D. (Eds.), Mechanisms of Global Climate Change at Millennial Time Scales. American Geophysical Union, p. 394.
Lisiecki, L.E., Raymo, M.E., 2007. Plio-Pleistocene climate evolution: trends and transitions in glacial cycle dynamics. Quat. Sci. Rev. 26, 56–69.
Marshall, S.J., Clark, P.U., 2002. Basal temperature evolution of North American ice sheets and implications for the 100-kyr cycle. Geophys. Res. Lett. 29, 4 pp.
Meckler, A.N., Schubert, C.J., Hochuli, P.A., Plessen, B., Birgel, D., Flower, B.P., Hinrichs, K.U., Haug, G.H., 2008. Glacial to Holocene terrigenous organic matter input to sediments from Orca Basin, Gulf of Mexico – a combined optical and biomarker approach. Earth Planet. Sci. Lett. 272, 251–263.
Moran, K., Backman, J., Brinkhuis, H., Clemens, S.C., Cronin, T., Dickens, G.R., Eynaud, F., Gattacceca, J., Jakobsson, M., Jordan, R.W., Kaminski, M., King, J., Koc, N., Krylov, A., Martinez, N., Matthiessen, J., McInroy, D., Moore, T.C., Onodera, J., O'Regan, M., Palike, H., Rea, B., Rio, D., Sakamoto, T., Smith, D.C., Stein, R., St John, K., Suto, I., Suzuki, N., Takahashi, K., Watanabe, M., Yamamoto, M., Farrell, J., Frank, M., Kubik, P., Jokat, W., Kristoffersen, Y., 2006. The Cenozoic palaeoenvironment of the arctic ocean. Nature 441, 601–605.
Münker, C., Weyer, S., Scherer, E., Mezger, K., 2001. Separation of high field strength elements (Nb, Ta, Zr, Hf) and Lu from rock samples for MC-ICPMS measurements. Geochem. Geophys. Geosyst. 2. Art. No.: 2001GC000183.
Nowell, G.M., Kempton, P.D., Noble, S.R., Fitton, J.G., Saunders, A.D., Mahoney, J.J., Taylor, R.N., 1998. High precision Hf isotope measurements of MORB and OIB by thermal ionisation mass spectrometry: insights into the depleted mantle. Chem. Geol. 149, 211–233.
Patchett, P.J., White, W.M., Feldmann, H., Kielinczuk, S., Hofmann, A.W., 1984. Hafnium rare-earth element fractionation in the sedimentary system and crustal recycling into the earths mantle. Earth Planet. Sci. Lett. 69, 365–378.
Paterson, W.S., 1972. Laurentide ice sheet – estimated volumes during late Wisconsin. Rev. Geophys. Space Phys. 10, 885–917.
Pattyn, F., 2010. Antarctic subglacial conditions inferred from a hybrid ice sheet/ice stream model. Earth Planet. Sci. Lett. 295, 451–461.
Peltier, W.R., 1994. Ice-age paleotopography. Science 265, 195–201.
Piepgras, D.J., Wasserburg, G.J., 1987. Rare earth element transport in the western North Atlantic inferred from Nd isotopic observations. Geochim. Cosmochim. Acta 51, 1257–1271.
Piotrowski, A.M., Lee, D.-C., Christensen, J.N., Burton, K.W., Halliday, A.N., Hein, J.R., Günther, D., 2000. Changes in erosion and ocean circulation recorded in the Hf isotopic compositions of North Atlantic and Indian Ocean ferromanganese crusts. Earth Planet. Sci. Lett. 181, 315–325.
Rasmussen, S.O., Andersen, K.K., Svensson, A.M., Steffensen, J.P., Vinther, B.M., Clausen, H.B., Siggaard-Andersen, M.L., Johnsen, S.J., Larsen, L.B., Dahl-Jensen, D., Bigler, M., Rothlisberger, R., Fischer, H., Goto-Azuma, K., Hansson, M.E., Ruth, U., 2006. A new Greenland ice core chronology for the last glacial termination. J. Geophys. Res.-Atmos. 111.
Rasmussen, S.O., Selerstad, I.K., Andersen, K.K., Bigler, M., Dahl-Jensen, D., Johnsen, S.J., 2008. Synchronization of the NGRIP, GRIP, and GISP2 ice cores across MIS 2 and palaeoclimatic implications. Quat. Sci. Rev. 27, 18–28.
Refsnider, K.A., Miller, G.H., Hillaire-Marcel, C., Fogel, M.L., Ghaleb, B., Bowden, R., 2012. Subglacial carbonates constrain basal conditions and oxygen isotopic composition of the Laurentide Ice Sheet over Arctic Canada. Geology 40, 135–138.
Reimer, P.J., Baillie, M.G.L., Bard, E., Bayliss, A., Beck, J.W., Blackwell, P.G., Ramsey, C.B., Buck, C.E., Burr, G.S., Edwards, R.L., Friedrich, M., Grootes, P.M., Guilderson, T.P., Hajdas, I., Heaton, T.J., Hogg, A.G., Hughen, K.A., Kaiser, K.F., Kromer, B., McCormac, F.G., Manning, S.W., Reimer, R.W., Richards, D.A., Southon, J.R., Talamo, S., Turney, C.S.M., van der Plicht, J., Weyhenmeye, C.E., 2009. INTCAL09 and MARINE09 radiocarbon calibration curves, 0–50,000 years cal BP. Radiocarbon 51, 1111–1150.
Rickli, J., Frank, M., Baker, A.R., Aciego, S., de Souza, G., Georg, R.B., Halliday, A.N., 2010. Hafnium and neodymium isotopes in surface waters of the eastern Atlantic Ocean: implications for sources and inputs of trace metals to the ocean. Geochim. Cosmochim. Acta 74, 540–557.
Rickli, J., Frank, M., Halliday, A.N., 2009. The hafnium-neodymium isotopic composition of Atlantic seawater. Earth Planet. Sci. Lett. 280, 118–127.
Rickli, J., Frank, M., Stichel, T., Georg, R.B., Vance, D., Halliday, A.N., 2013. Controls on the incongruent release of hafnium during weathering of metamorphic and sedimentary catchments. Geochim. Cosmochim. Acta 101, 263–284.
Rickli, J., Gutjahr, M., Vance, D., Fischer-Gödde, M., Hillenbrand, C.-D., Kuhn, G., 2014. Neodymium and hafnium boundary contributions to seawater along the West Antarctic continental margin. Earth Planet. Sci. Lett. 394, 99–110.
Roberts, N.L., Piotrowski, A.M., McManus, J.F., Keigwin, L.D., 2010. Synchronous deglacial overturning and water mass source changes. Science 327, 75–78.
Robinson, L.F., Adkins, J.F., Keigwin, L.D., Southon, J., Fernandez, D.P., Wang, S.L., Scheirer, D.S., 2005. Radiocarbon variability in the western North Atlantic during the last deglaciation. Science 310, 1469–1473.
Robinson, L.F., Noble, T.L., McManus, J.F., 2008. Measurement of adsorbed and total Th-232/Th-230 ratios from marine sediments. Chem. Geol. 252, 169–179.
Ruddiman, W.F., 1977. Late Quaternary deposition of ice-rafted sand in subpolar North Atlantic (lat 40 degrees to 65 degrees N). Geol. Soc. Am. Bull. 88, 1813–1827.
Ryan, W.B.F., Carbotte, S.M., Coplan, J.O., O'Hara, S., Melkonian, A., Arko, R., Weissel, R.A., Ferrini, V., Goodwillie, A., Nitsche, F., Bonczkowski, J., Zemsky, R., 2009. Global multi-resolution topography synthesis. Geochem. Geophys. Geosyst. 10. Art. No.: Q03014.
Scherer, E., Munker, C., Mezger, K., 2001. Calibration of the lutetium-hafnium clock. Science 293, 683–687.
Shaw, J., Piper, D.J.W., Fader, G.B.J., King, E.L., Todd, B.J., Bell, T., Batterson, M.J., Liverman, D.G.E., 2006. A conceptual model of the deglaciation of Atlantic Canada. Quat. Sci. Rev. 25, 2059–2081.
Sionneau, T., Bout-Roumazeilles, V., Flower, B.P., Bory, A., Tribovillard, N., Kissel, C., Van Vliet-Lanoe, B., Serrano, J.C.M., 2010. Provenance of freshwater pulses in the Gulf of Mexico during the last deglaciation. Quat. Res. 74, 235–245.

Stichel, T., Frank, M., Rickli, J., Haley, B.A., 2012a. The hafnium and neodymium isotope composition of seawater in the Atlantic sector of the Southern Ocean. Earth Planet. Sci. Lett. 317–318, 282–294.
Stichel, T., Frank, M., Rickli, J., Hathorne, E.C., Haley, B.A., Jeandel, C., Pradoux, C., 2012b. Sources and input mechanisms of hafnium and neodymium in surface waters of the Atlantic sector of the Southern Ocean. Geochim. Cosmochim. Acta 94, 22–37.
van de Flierdt, T., Frank, M., Lee, D.C., Halliday, A.N., 2002. Glacial weathering and the hafnium isotope composition of seawater. Earth Planet. Sci. Lett. 198, 167–175.
van de Flierdt, T., Frank, M., Lee, D.C., Halliday, A.N., Reynolds, B.C., Hein, J.R., 2004. New constraints on the sources and behavior of neodymium and hafnium in seawater from Pacific Ocean ferromanganese crusts. Geochim. Cosmochim. Acta 68, 3827–3843.
van de Flierdt, T., Goldstein, S.L., Hemming, S.R., Roy, M., Frank, M., Halliday, A.N., 2007. Global neodymium–hafnium isotope systematics – revisited. Earth Planet. Sci. Lett. 259, 432–441.
Vance, D., Teagle, D.A.H., Foster, G.L., 2009. Variable Quaternary chemical weathering fluxes and imbalances in marine geochemical budgets. Nature 458, 493–496.
Vautravers, M.J., Shackleton, N.J., Lopez-Martinez, C., Grimalt, J.O., 2004. Gulf Stream variability during marine isotope stage 3. Paleoceanography 19. Art. No. PA2011.
Vervoort, J.D., Patchett, P.J., Blichert-Toft, J., Albarède, F., 1999. Relationship between Lu–Hf and Sm–Nd isotopic systems in the global sedimentary system. Earth Planet. Sci. Lett. 168, 79–99.
Vervoort, J.D., Plank, T., Prytulak, J., 2011. The Hf–Nd isotopic composition of marine sediments. Geochim. Cosmochim. Acta 75, 5903–5926.
Wacker, L., Lippold, J., Molnár, M., Schulz, H., 2013. Towards single-foraminifera-dating with a gas ion source. Nucl. Instrum. Methods 294, 307–310.
White, W.M., Patchett, P.J., BenOthman, D., 1986. Hf isotope ratios of marine sediments and Mn nodules: evidence for a mantle source of Hf in seawater. Earth Planet. Sci. Lett. 79, 46–54.
Zimmermann, B., Porcelli, D., Frank, M., Andersson, P.S., Baskaran, M., Lee, D.C., Halliday, A.N., 2009a. Hafnium isotopes in Arctic Ocean water. Geochim. Cosmochim. Acta 73, 3218–3233.
Zimmermann, B., Porcelli, D., Frank, M., Rickli, J., Lee, D.C., Halliday, A.N., 2009b. The hafnium isotope composition of Pacific Ocean water. Geochim. Cosmochim. Acta 73, 91–101.